Available online at www.sciencedirect.com
SCIENCE DIRECT®
Geochimica et Cosmochimica Acta 70 (2006) 71–89
Geochimica
www.elsevier.com/locate/gca

Time scale and conditions of weathering under tropical climate: Study of the Amazon basin with U-series

A. Dosseto [a,*], B. Bourdon [a], J. Gaillardet [a], C.J. Allègre [a], N. Filizola [b]

[a] *Laboratoire de Géochimie et Cosmochimie, IPGP-CNRS UMR 7579, 4 Place Jussieu, 75252 Paris cedex 05, France*
[b] *IRD-LMTG, Université Paul Sabatier, 38 rue des 36 ponts, 31400 Toulouse, France*

Received 12 October 2004; accepted in revised form 23 June 2005

Abstract

The Rio Solimões/Amazonas (Amazon River) and its major tributaries have been analyzed for U-series nuclides. ^{238}U–^{234}U–^{230}Th–^{226}Ra disequilibria have been measured in the dissolved (<0.2 μm) and suspended loads (>0.2 μm) as well as bed sands. U-series disequilibria are closely related to major and trace element compositions and therefore reflect elemental fractionation during chemical weathering. Moreover, while the dissolved load records present-day weathering, suspended particles integrate the erosion history over much longer time scales (>100 ka). Lowland rivers are characterized by long time scales of chemical erosion ($\geqslant$100 ka) resulting in a high weathering intensity. Moreover, exchange between suspended particles and the dissolved load may explain the U-series signature for these rivers. By combining U-series and Pb isotopes in suspended particles, we show that erosion in the Rio Madeira basin occurred as a multi-step process, whereby the pristine continental crust was eroded several hundreds of Ma ago to produce sediments that have then been integrated in the Cordillera by crustal shortening and are currently eroded. In contrast, recent erosion of a pristine crust is more likely for the Rio Solimões/Amazonas (<10 ka). The suspended particles of the rivers draining the Andes (Solimões/Amazonas, Madeira) suggest time scales of weathering ranging between 4 and 20 ka. This indicates that suspended particles transported by those rivers are not stored for long periods in the Andean foreland basin and the tropical plain. The sediments delivered to the ocean have resided only a few ka in the Amazon basin (6.3 ± 1 ka for the Rio Amazonas at Óbidos). Nevertheless, a large fraction of the sediments coming out from the Andes are trapped in the foreland basin and may never reach the ocean. Erosion in the Andes is not operating in steady state. U-series systematics shows unambiguously that rivers are exporting a lot more sediments than predicted by steady-state erosion and that is a consequence of soil destruction greater than production. By relating this observation to the short time scales of weathering inferred for the Andes (a few ka), it appears that the erosion regime has been recently perturbed, resulting in high denudation rates. A possible explanation would be the increase in precipitation less than 5 ka proposed by recent paleoclimatic studies. Our results indicate that erosion responds rapidly to high-frequency climatic fluctuations.

1. Introduction

The continental crust is destroyed via two main mechanisms of erosion. First, chemical weathering removes the most soluble elements from the rock and the residue left behind forms a soil. Second, physical denudation transports the soils and rocks. Erosion products, solutes derived from chemical weathering and sediments from soil destruction, are exported by rivers to the oceans. Previous studies have used the composition of riverine material to estimate, at the scale of the river basin, continental erosion rates (e.g., Gaillardet et al., 1995, 1997, 1999a,b; Martin and Meybeck, 1979; Milliman and Meade, 1983) and/or fluxes of CO_2 consumption through silicate weathering, because it acts as a sink for atmospheric CO_2 (e.g., Gaillardet et al., 1997, 1999a,b). All these studies are based on the assumption that erosion operates at steady state, i.e., there is a perfect balance between the mass of rock converted into soil

* Corresponding author. Present address: GEMOC Key Centre, Department of Earth and Planetary Sciences, Macquarie University, NSW2109 Sydney, Australia. Fax: +61 2 9850 8943.
E-mail address: adosseto@els.mq.edu.au (A. Dosseto).

0016-7037/$ - see front matter © 2005 Elsevier Inc. All rights reserved.
doi:10.1016/j.gca.2005.06.033

and the mass of erosion products exported by the river. Using major and trace element compositions of river dissolved and suspended loads from the Amazon and Congo basins, Gaillardet et al. (1995, 1997) have shown that this hypothesis may be valid for lowland rivers but is not so for rivers draining the Andes. However, in their model, they had used an average upper crust composition (Taylor and McLennan, 1985) for the composition of the bedrock that may not be valid for sub-basins of the Amazon. As a consequence, it was difficult to be conclusive about the actual steady state of erosion.

Uranium-series are potentially very useful to address this question as after 1 Ma, all nuclides in a decay chain are in secular equilibrium (all parent–daughter activity ratios equal 1). This condition should be verified for the bedrock, as it is, in most cases, older than 1 Ma. Thus, the U-series composition of the bedrock and the initial conditions of weathering are known.

There are several issues where a better knowledge of the time scales involved in erosion processes is required: (1) to understand the evolution of continental masses, it is important to have an estimate of the time scale of erosion relative to mountain-building and crustal genesis; (2) because chemical weathering pumps CO_2 from the atmosphere, this process plays a role in the Earth's climate regulation. Hence, if it is possible to determine how external forcings (tectonic, climatic or anthropic) with differing time scales modify the erosion regime, we should be able to better appreciate their impact on the evolution of atmospheric CO_2 contents with time; (3) finally, another important issue is to understand how sediments are transported through a basin, i.e., for how long they are stored and how much time is needed for them to reach the ocean. To achieve these objectives, U-series isotopes provide a powerful tool since the fractionation in the decay chains (=radioactive disequilibrium) is time-dependent. Once a disequilibrium is produced (i.e., the parent–daughter activity ratio deviates from unity), the system returns to secular equilibrium on time scales dictated by the daughter nuclide half-life. ^{234}U–^{238}U, ^{230}Th–^{238}U, and ^{226}Ra–^{230}Th systems record fractionations younger than 1 Ma, 300, and 10 ka, respectively (Figs. 2A and B; Chabaux et al., 2003; Osmond and Ivanovich, 1992).

During chemical weathering, U and Ra are generally thought to be more mobile than Th (Langmuir, 1978; Langmuir and Herman, 1980; Langmuir and Riese, 1985). The dissolved phase is then expected to show ($^{230}Th/^{238}U$) activity ratios <1 ($^{226}Ra/^{230}Th$) > 1 and the opposite in solid phases (ratios in parentheses denote activity ratios throughout this paper). Additionally, because of recoil effects, ^{234}Th can be ejected from the solid and the rapid decay in ^{234}U ($T_{234Th} = 24$ d) can induce ($^{234}U/^{238}U$) ratios >1 in the waters and <1 in the residues of weathering (Osmond and Cowart, 1982). It is generally assumed that during weathering heavy isotopes like ^{230}Th and ^{232}Th do not fractionate. However, the ($^{230}Th/^{232}Th$) in residual solids may decrease because of the decay of excess ^{230}Th. Their ($^{230}Th/^{232}Th$) will significantly deviate from the initial bedrock value only if the removal of U is older than the half-life of ^{230}Th (75 ka) (Fig. 2C).

Previous U-series studies of riverborne material (see Chabaux et al., 2003 for a recent review) have focused on the contribution of rivers to the seawater U budget (e.g., Borole et al., 1982; Palmer and Edmond, 1993; Pande et al., 1994; Sarin et al., 1990), the behavior of U-series isotopes during weathering and transport in the river (e.g., Andersson et al., 1998; Plater et al., 1992; Porcelli et al., 1997, 2001), or the sources of dissolved flux, in particular groundwater contributions (Chabaux et al., 2001; Riotte and Chabaux, 1999; Riotte et al., 2003). Recently, Vigier et al. (2001) have used U-series isotopes to show that the time scale characteristic of weathering in the Mackenzie basin is ~10–30 ka. They suggest that this value indicates a recent change in the conditions of erosion probably linked to the inception of the last deglaciation. A similar approach is adopted in the present study, where ^{238}U–^{234}U–^{230}Th–^{226}Ra nuclides have been measured in the dissolved load, suspended particles, and bed sands based on sampling of the Amazon mainstream at different locations and of its major tributaries.

The aims of this study were: (1) to use U-series disequilibria to characterize the different weathering regimes encountered in the Amazon basin, (2) to constrain the time scales and conditions of weathering in the tropical plain and Precambrian shields on the one hand (lowlands) and the Andes on the other hand, by considering separately rivers draining these regions.

2. The Amazon basin

The Amazon basin is the largest watershed in the world (ca. 6×10^6 km^2). With an average annual discharge of 2.09×10^5 m^3/s (Molinier et al., 1995) and a sediment flux of 600×10^6 t/an (Filizola, 1999), the Amazon River represents the largest water discharge and the third largest sediment flux to the ocean in the world. Hence, constraints about mechanisms of erosion for this basin may provide a good picture of continental erosion at a global scale. The Amazon basin is composed of several morphostructural domains (Fig. 1) and thus offers the opportunity of studying erosion in various tectonic contexts: active orogene (the Andean Cordillera), intra-continental troughs (Amazon and Subandean Troughs), and stable cratons. Moreover, various weathering regimes are found (Stallard and Edmond, 1983): erosion of thick, severely weathered profiles in the lowlands and thin soils constituted of poorly weathered material in the Andes. This makes the Amazon basin representative of the diversity of weathering regimes around the world.

Waters of the Amazon basin have been previously classified into three groups (Sioli, 1968; Stallard and Edmond, 1983): (1) white waters originating from the Andes, which have high dissolved and suspended loads (e.g., Rio Solimões/Amazonas and Rio Madeira); (2) clear waters,

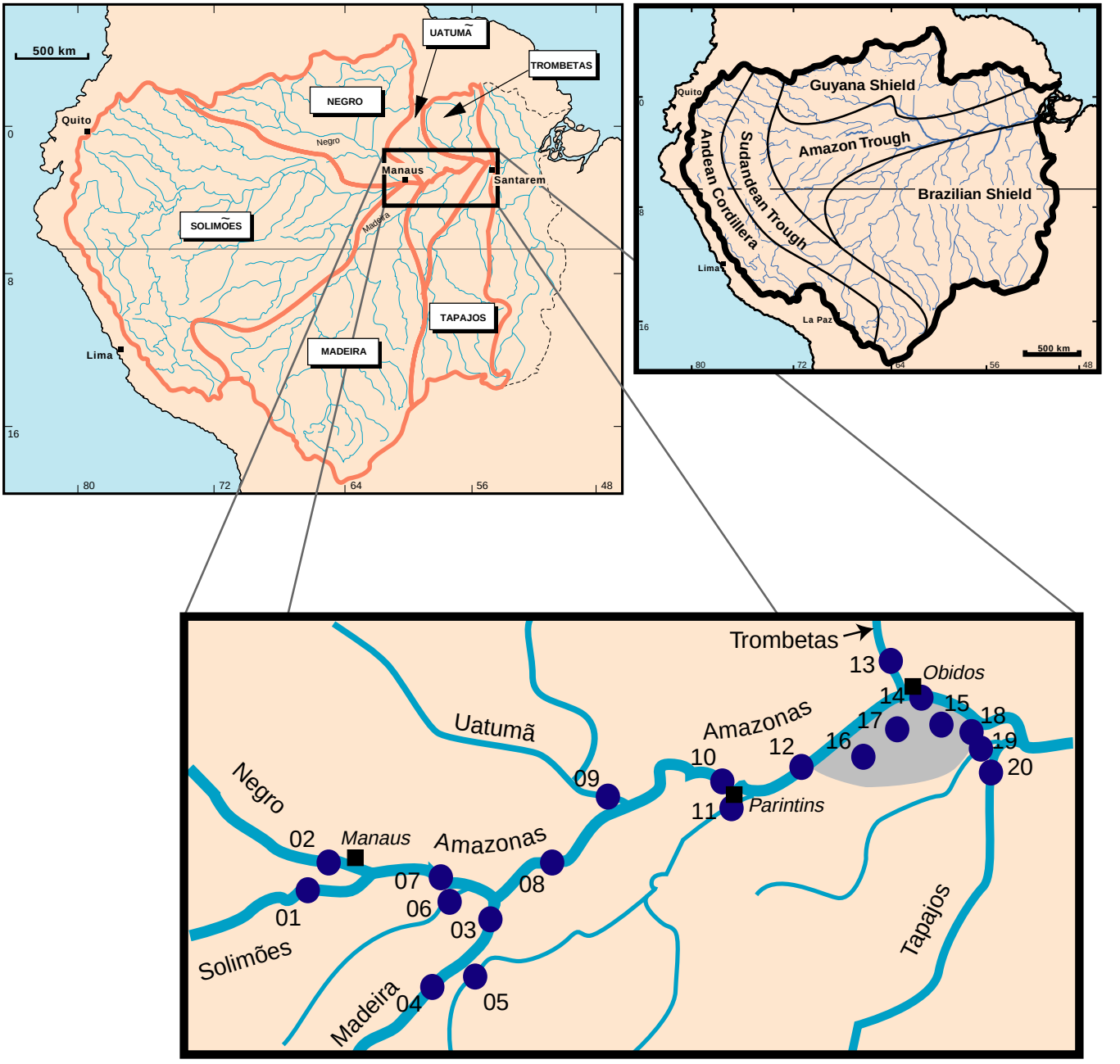

Fig. 1. Map of the Amazon basin with sampling locations (dots). Numbers on the map refer to the two last digits of sample names in Tables 1–4. The light gray area is the large floodplain named Lago Grande de Curuai. Squares are town locations (names given in italics). Major morphostructural zones are: (1) the Andean Cordillera, (2) the Subandean Trough, (3) the Amazon Trough, and (4) the Precambrian shields (after Stallard and Edmond, 1983).

with low dissolved and suspended loads (e.g., Rio Tapajós); and (3) black waters, with low dissolved and suspended loads, characterized by a brown coloration due to abundant organic acids (e.g., Rio Negro). White waters are typical of rivers draining the Andean Cordillera in the upper part of their basin. Clear and black water types are both encountered in lowlands and drain Precambrian shields and Tertiary sediments from the Amazon Trough. Black waters can be distinguished from clear waters because they drain low forested area (Northwest), which are characterized by white podzolitic soils dominated by quartz, kaolinite, and aluminum oxides. Clear waters drain savannas with soils richer in kaolinite, iron, and aluminum oxides (Stallard and Edmond, 1983, and references therein). In the lowland regions, cation-poor waters (clear and black waters) are a consequence of the drainage of extensively weathered terranes where most of the soluble elements have been previously removed. Moreover, these regions are characterized by low physical erosion rate, with very low suspended loads in river waters, as a consequence of smooth relief and thick weathering profiles (Guyot, 1993).

3. Sampling and analytical procedures

River waters were sampled in May 2001, in collaboration with the HYBAM project (Hydrology and Geochemistry of the Amazon basin) conducted by IRD (Institut de Recherche pour le Développement). This period of the year corresponds to the high water stage for Rio Solimões/Amazonas (Amazon River) and the end of the high water stage for Rio Madeira. Major tributaries of the Amazon have been sampled: Rio Madeira, which drains the Bolivian Andes and the Brazilian shield; Rio Negro and Rio Trombetas, lowland rivers from the Northern basin which drain the Guyana shield; and Rio Tapajós, a lowland river from the Southern basin which drains exclusively the Brazilian shield. Minor tributaries have also been sampled: Rio Uatumã, a lowland river from the Northern basin; Rio Abacaxi, Paraná Madeirinha, Paraná do Ramos, and Rio Arapiuns (a tributary of the Rio Tapajós), lowland rivers from the Southern basin, flowing in the Amazon Trough. The Amazon River has been sampled at six different locations: before the confluence with Rio Negro (where it is named 'Rio Solimões') and after (where it becomes 'Rio Amazonas'). Finally, several 'lakes' and an artesian well from the large floodplain 'Lago Grande do Curuai' have also been sampled.

Water samples were collected in the middle of the stream, at about 1 m depth, and filtered at 0.2 μm by frontal filtration (sampling locations given in Fig. 1). pH and alkalinity (acid–base titration of HCO_3^-) were determined in the field. The filtrates were stored in acid-washed polypropylene bottles and acidified with distilled nitric acid to pH 2. Suspended particles were collected from the filter, dried, and crushed.

In the dissolved load, major element concentrations (Na, K, Mg, Ca, Cl, NO_3, and SO_4) were measured by ion chromatography (Dionex 300) with a precision of ±1–3%, and trace element abundances were determined by inductively coupled plasma-mass spectrometry (ICP-MS) at the University of Toulouse, on a VG PlasmaQuad II+, with a precision of ±2–6% (Table 1). For suspended particles, major elements were analyzed by ICP-AES and trace elements by ICP-MS (CRPG Nancy) after fusion of samples with lithium borate and dissolution in ultrapure HNO_3 (Table 2).

About 200 ml of filtrate was accurately weighted and spiked with ^{236}U, ^{229}Th, and ^{228}Ra for U, Th, and ^{226}Ra concentration measurements. They were then evaporated and re-dissolved in HNO_3 7.5 N before elemental separation. For suspended particles and sands, approximately 50 mg of material was spiked and dissolved in a mixture of HF, HNO_3, and $HClO_4$. After a first stage of H_2SiF_6 evaporation at 80 °C, $HClO_4$ was evaporated at higher temperature (>140 °C) and the residue was re-dissolved in $HNO_3 + H_3BO_3$. The solution was then evaporated and re-dissolved in nitric acid. This last stage was repeated twice, in order to eliminate perchlorates, before loading on ion chromatography columns. Separation of radium was performed following the procedure described in

Table 1
Major and trace element concentrations in the dissolved load

River name	Sample name	pH	Na	K	Mg	Ca	Cl	NO_3	SO_4	HCO_3	TDS	Al	Ti	Sm
Rivers draining the Andes (white waters)														
Solimões	AM6/1-01	7.38	2.76	0.94	1.19	9.47	2.80	1.00	2.82	33.5	54.5	3.0	89	13.5
Amazonas 07-LB (before Madeira, near left bank)	AM6/1-07 25%	7.30	1.96	0.73	0.83	6.21	1.93	0.15	1.87	23.3	37.0	18.9	165	35.0
Amazonas 07-M (before Madeira, river middle)	AM6/1-07 50%	7.30	2.43	0.88	1.06	7.97	2.50	—	2.36	30.0	47.2	6.6	101	23.2
Amazonas 07-RB (before Madeira, near right bank)	AM6/1-07 75%	7.30	2.50	0.90	1.10	8.19	2.37	—	2.40	31.1	48.6	6.2	172	21.0
Amazonas 08 (after Madeira)	AM6/1-08	7.11	2.26	0.93	1.16	7.16	1.91	0.02	2.73	28.0	44.2	5.4	105	20.5
Amazonas 10 (at Parintins)	AM6/1-10	6.96	1.97	0.86	1.02	6.20	1.61	0.02	2.41	24.5	38.5	9.8	113	31.2
Amazonas 12 (after Parintins)	AM6/1-12	7.14	1.79	0.82	1.00	5.62	1.37	0.01	2.26	22.6	35.5	—	—	—
Amazonas 14 (at Óbidos)	AM6/1-14	7.20	1.91	0.85	1.04	5.98	1.52	0.05	2.39	24.1	37.8	—	—	—
Madeira 03 (at Uricurituba)	AM6/1-03	7.20	1.65	1.20	1.64	4.29	0.40	0.05	5.40	19.8	34.4	3.9	108	17.4
Madeira 04 (at Fazenda Vista Alegre)	AM6/1-04	7.67	1.69	1.20	1.63	4.32	0.43	0.04	5.62	19.3	34.3	4.6	162	20.5
Lowland rivers (black and clear waters)														
Negro	AM6/1-02	4.38	0.27	0.23	0.06	0.17	0.20	0.55	0.15	0.8	2.4	137.3	417	45.4
Abacaxi	AM6/1-05	5.82	0.22	0.41	0.12	0.19	0.20	0.04	0.11	1.8	3.1	37.3	3	15.4
Paraná Madeirinha	AM6/1-06	7.24	2.47	0.90	1.09	8.20	2.40		2.41	31.1	48.6	3.9	86	20.0
Uatumã	AM6/1-09	6.58	1.04	0.73	0.43	2.26	0.77	0.03	0.74	10.5	16.5	30.0	70	37.3
Paraná do Ramos	AM6/1-11	6.80	0.93	0.59	0.61	2.46	0.63	0.05	1.41	10.9	17.6	12.5	47	23.7
Trombetas	AM6/1-13	6.30	0.89	0.68	0.19	0.44	0.53	0.20	0.21	4.3	7.4	34.1	27	35.9
Arapiuns	AM6/1-19	6.80	0.59	0.39	0.21	0.55	0.67	0.04	0.21	3.3	5.9	20.2	3	22.6
Tapajós	AM6/1-20	6.83	0.76	0.87	0.43	0.94	0.37	0.60	0.15	7.0	11.1	—	—	—
Floodplain "Lago Grande do Curuai"														
Lago do Salé outlet	AM6/1-15	7.26	1.60	0.68	0.96	5.08	1.17		1.95	20.9	32.4	3.4	—	9.5
Artesian well A28	AM6/1-16	6.52	7.33	1.06	0.56	0.57	0.58		0.56	23.9	34.6	0.8	—	0.2
Lago Curumcuri	AM6/1-17	7.16	1.36	0.60	0.79	4.17	1.06	0.16	1.57	17.1	26.8	—	—	—
Lago Grande do Curuai outlet	AM6/1-18	7.12	1.66	0.74	1.09	5.45	1.17	0.06	2.28	22.4	34.8	—	—	—

All concentrations are in ppm, except for Al (in ppb), Ti and Sm (in ppt). HCO_3 concentration is alkalinity measured in the field.

Table 2
Major and trace element concentrations in the suspended particles

River name	Sample name	SiO_2	Al_2O_3	Fe_2O_3	MnO	MgO	CaO	Na_2O	K_2O	TiO_2	P_2O_5	LOI	Sm
Rivers draining the Andes													
Solimões	AM6/1-01	52.3	18.5	8.3	0.090	1.62	1.33	0.900	2.26	0.790	0.270	13.5	7.94
Madeira 03	AM6/1-03	51.6	22.3	9.1	0.075	1.55	0.50	0.573	3.59	0.876	0.253	11.1	9.71
Madeira 04	AM6/1-04	53.3	22.0	8.9	0.072	1.55	0.45	0.609	3.66	0.923	0.245	10.3	9.79
Amazonas 07-LB	AM6/1-07 25%	55.9	18.0	7.8									8.04
Amazonas 07-RB	AM6/1-07 75%	55.9	18.0	7.8	0.124	1.64	1.35	1.09	2.36	0.906	0.257	12.0	7.83
Amazonas 10	AM6/1-10	53.2	20.3	8.6	0.089	1.55	0.94	0.767	2.81	0.880	0.272	12.2	9
Amazonas 12	AM6/1-12	54.8	19.4	8.3	0.090	1.54	0.91	0.820	2.80	0.930	0.250	11.4	7.95
Amazonas 14	AM6/1-14	53.7	19.8	8.3	0.079	1.52	0.91	0.783	2.78	0.883	0.257	12.7	7.62
Lowland river													
Paraná do Ramos	AM6/1-11	59.9	16.6	7.3	0.082	1.33	0.68	0.866	2.66	0.945	0.203	9.9	5.16

All concentrations are in wt%, except for Sm (in ppm).

(Claude-Ivanaj, 1997), while separation of Th and U followed a procedure adapted from Manhès (1981). U, Th, and ^{226}Ra concentrations were determined by thermo-ionization mass spectrometry (TIMS) using an isotope dilution technique. $^{234}U/^{238}U$ and $^{230}Th/^{232}Th$ ratios were measured by TIMS, except for Th isotopes in the dissolved phase, which were determined by plasma ionization mass spectrometry, using a Nu Plasma Multi-Collector ICP-MS at the Open University, UK (Turner et al., 2001). $^{230}Th/^{232}Th$ ratios in suspended particles and sands as well as Th, U concentrations and $^{234}U/^{238}U$ ratios in waters, suspended and bedload sediments were determined on a ThermoFinnigan Triton at IPGP. ^{226}Ra concentrations were measured on a Finnigan MAT262 at IPGP. Internal analytical uncertainty for ($^{226}Ra/^{230}Th$) activity ratios in the dissolved phase is variable as a consequence of the difficulty in obtaining accurate measurements for some samples. External analytical uncertainty has been estimated for concentration measurements, by replicate analysis of the samples. In the dissolved phase, it amounts to 0.13 and 1.7%, respectively, for U and ^{226}Ra concentrations. In the suspended particles, it is estimated for U, Th, and ^{226}Ra concentrations, respectively, to 0.7, 1.3, and 0.10%. The internal analytical uncertainties for $^{234}U/^{238}U$ and $^{230}Th/^{232}Th$ ratios in the dissolved, suspended, and bed loads are reported in Tables 3–5 for each sample. The isotope dilution technique for U, Th, and ^{226}Ra concentrations has been checked for suspended particles and bed sands by analyzing a rock standard with concentrations similar to those of the samples (AThO; values taken from Peate et al., 2001). Measured concentrations in AThO are: $[Th] = 7.50 \pm 0.14$ ppm ($n = 3$; 2σ error), $[U] = 2.25 \pm 0.02$ ppm

Table 3
U-series data for the dissolved phase of the Amazon River at different locations and its major tributaries

River name	Sample name	U	Th	Ra	($^{234}U/^{238}U$)	($^{230}Th/^{238}U$)	($^{226}Ra/^{230}Th$)	($^{238}U/^{232}Th$)	($^{230}Th/^{232}Th$)
Rivers draining the Andes									
Solimões	AM6/1-01	57.8	8.3	13.1	1.23 ± 1	0.0577 ± 6	19.5 ± 3	12.4 ± 1	0.714 ± 4
Amazonas 07-LB	AM6/1-07 25%	52.3	33.4	19.3	1.19 ± 1	0.172 ± 6	8.02 ± 2	3.70 ± 5	0.637 ± 2
Amazonas 07-M	AM6/1-07 50%	50.1	29.0	15.2	1.22 ± 1			4.74 ± 1	
replicate		50.0		15.0					
Amazonas 07-RB	AM6/1-07 75%	48.8	18.5	14.4	1.23 ± 1	0.0959 ± 3	11.2 ± 1	6.43 ± 1	0.616 ± 2
Amazonas 08	AM6/1-08	48.2	15.9	14.0	1.23 ± 3	0.0994 ± 9	12.2 ± 1	6.41 ± 3	0.637 ± 2
Amazonas 10	AM6/1-10	50.8	28.3	14.0	1.23 ± 2	0.112 ± 1	12.2 ± 1	5.41 ± 2	0.605 ± 2
Amazonas 12	AM6/1-12	45.7	21.2		1.27 ± 3	0.124 ± 1	9.4 ± 4	5.81 ± 1	0.721 ± 5
Amazonas 14	AM6/1-14	52.2	27.5	22.3	1.23 ± 1	0.1425 ± 2	10.2 ± 3	4.93 ± 1	0.702 ± 5
Madeira 03	AM6/1-03	29.0	13.3	14.5	1.27 ± 1	0.0937 ± 7	15.6 ± 6	6.57 ± 3	0.616 ± 2
Madeira 04	AM6/1-04	32.7	12.2	14.3	1.26 ± 3	0.078 ± 1	18.1 ± 7	7.35 ± 3	0.573 ± 8
Lowland rivers									
Negro	AM6/1-02	25.2	85.8	35.4	0.99 ± 1	0.559 ± 6	8.2 ± 3	0.790 ± 4	0.442 ± 5
Uatumã	AM6/1-09	39.7	83.5		1.14 ± 1	0.332 ± 1		1.43 ± 2	0.476 ± 1
Trombetas	AM6/1-13	37.5	107.6	49.7	1.04 ± 1	0.390 ± 5	11.1 ± 3	0.938 ± 1	0.366 ± 4
Paraná do Ramos	AM6/1-11	27.7	16.5		1.39 ± 1			4.5 ± 1	
Arapiuns	AM6/1-19	24.4	18.2	32.6	2.04 ± 4			3.59 ± 7	
Tapajós	AM6/1-20	27.3	29.4	31.5	1.34 ± 1	0.247 ± 4	18 ± 1	2.89 ± 2	0.713 ± 5
Floodplain									
Lago Grande do Curuai outlet	AM6/1-18	39.1		1.8	1.23 ± 1				

U and Th concentrations are in ng/L, Ra in fg/L. Internal analytical uncertainties are given on the last digit at the 2σ level.

Table 4
U-series data for the suspended particles of the Amazon River at different locations and its major tributaries

River name	Sample name	U	Th	Ra	(^{234}U/^{238}U)	(^{230}Th/^{238}U)	(^{226}Ra/^{230}Th)	(^{238}U/^{232}Th)	(^{230}Th/^{232}Th)
Rivers draining the Andes									
Solimões	AM6/1-01	3.42	14.8	1.28	0.99 ± 2	1.27 ± 3	0.86 ± 4	0.70 ± 1	0.885 ± 3
Amazonas 07-LB	AM6/1-07 25%	3.55	14.6	1.35	0.99 ± 2	1.12 ± 1	1.00 ± 1	0.733 ± 6	0.819 ± 2
Amazonas 07-RB	AM6/1-07 75%	3.26	13.5	1.25	1.00 ± 1	1.17 ± 3	0.96 ± 4	0.73 ± 1	0.855 ± 8
Amazonas 10	AM6/1-10	3.32	15.8	1.39	1.00 ± 1	1.20 ± 2	1.02 ± 3	0.636 ± 8	0.762 ± 5
Amazonas 12	AM6/1-12	3.27	15.4	1.34	0.979 ± 5	1.18 ± 1	1.01 ± 2	0.642 ± 4	0.758 ± 2
Amazonas 14	AM6/1-14	3.03	14.8	1.35	1.00 ± 1	1.32 ± 2	0.99 ± 4	0.618 ± 7	0.816 ± 3
Madeira 03	AM6/1-03	3.27	17.8	1.30	0.996 ± 6	1.17 ± 2	0.99 ± 3	0.553 ± 4	0.647 ± 6
Madeira 04	AM6/1-04	3.42	18.4	1.37	1.00 ± 1	1.16 ± 2	1.00 ± 1	0.559 ± 5	0.653 ± 4
replicate			18.2	1.37			1.01 ± 1		0.658 ± 3
Lowland rivers									
Negro	AM6/1-02	3.21	14.3	2.37	1.033 ± 3	0.262 ± 3	8.3 ± 2	0.675 ± 5	0.177 ± 1
replicate		3.23			1.022 ± 5				
Uatumã	AM6/1-09	3.23	17.5	2.56	1.02 ± 2	1.27 ± 3	1.82 ± 8	0.56 ± 1	0.710 ± 6
Trombetas	AM6/1-13	4.13	23.2	3.65	1.027 ± 3	0.713 ± 1	3.6 ± 1	0.542 ± 5	0.383 ± 4
Paraná do Ramos	AM6/1-11	3.11	17.8	1.83	0.99 ± 1	1.50 ± 4	1.14 ± 6	0.525 ± 9	0.790 ± 9

U and Th concentrations are in ppm, Ra in pg/g. Internal analytical uncertainties are given on the last digit at the 2σ level.

Table 5
Data comparison between suspended particles (SP) and bed sediments (BD)

River name	Solimões		Madeira 03		Amazonas 10	
	SP	BD	SP	BD	SP	BD
U	3.42	2.86	3.27	1.24	3.32	1.79
Th	14.8	12.25	17.8	6.31	15.8	8.33
^{226}Ra	1.28	0.607	1.30	0.412	1.39	0.615
(^{234}U/^{238}U)	0.99 ± 2	0.985 ± 3	0.996 ± 6	1.03 ± 2	1.00 ± 1	1.00 ± 1
(^{230}Th/^{238}U)	1.27 ± 3	1.10 ± 1	1.17 ± 2	1.21 ± 1	1.20 ± 2	1.09 ± 2
(^{226}Ra/^{230}Th)	0.86 ± 4	0.901 ± 8	0.99 ± 3	0.80 ± 1	1.02 ± 3	0.92 ± 2
(^{238}U/^{232}Th)	0.70 ± 1	0.706 ± 3	0.553 ± 4	0.592 ± 3	0.636 ± 8	0.649 ± 7
(^{230}Th/^{232}Th)	0.885 ± 3	0.779 ± 2	0.647 ± 6	0.716 ± 3	0.762 ± 5	0.710 ± 2
SiO_2	52.3	64.9	51.6	89.0	53.2	81.1
Al_2O_3	18.5	15.4	22.3	4.9	20.3	7.1
Fe_2O_3	8.27	5.98	9.11	2.45	8.60	4.41
MgO	1.62	1.55	1.55	0.28	1.55	0.94
CaO	1.33	1.24	0.50	0.15	0.94	1.08
Na_2O	0.90	1.35	0.57	0.44	0.77	1.00
K_2O	2.26	2.16	3.59	1.17	2.81	1.33
TiO_2	0.79	0.88	0.88	0.30	0.88	1.13

Data for Rio Madeira and Rio Amazonas are from samples taken, respectively, at Urucurituba (AM6/1-03) and Parintins (AM6/1-10). All major element data are in wt%, U and Th concentrations are in ppm, and ^{226}Ra in pg/g. Internal analytical uncertainties are given on the last digit at the 2σ level.

($n = 4$; 2σ error), and [^{226}Ra] = 842 ± 6 fg/g ($n = 3$; 2σ error), and deviate from the published values by 0.9, 0.4, and 0.3%, respectively. ^{230}Th/^{232}Th measurements on the Triton and the Nu Plasma were checked by analyzing a standard solution, Th S1 (Claude-Ivanaj et al., 1998). The averages of five analyses on the Triton (^{230}Th/^{232}Th = $5.51 \times 10^{-6} \pm 0.02$; 2$\sigma$ error) and seven analyses on the Nu Plasma ($5.46 \times 10^{-6} \pm 0.04$; 2$\sigma$ error) deviate from the published value by 3.6 and 4.8‰, respectively. Similarly, ^{234}U/^{238}U determination on the Triton was checked by analyzing the standard solution NBS 960 (Cheng et al., 2000). The average of 11 analysis (^{234}U/^{238}U = $5.294 \times 10^{-5} \pm 0.009$; 2$\sigma$ error) deviates from the published value by 4.5‰.

4. Results

4.1. Dissolved phase

U-series data for the dissolved phase are presented in Table 3. U concentrations show a relatively narrow range with values from 24.4 (Rio Arapiuns) to 57.8 ng/L (Rio Solimões). The lowest values are observed for lowland rivers and Rio Madeira, the highest for the Amazon River (Solimões/Amazonas). The U content of the Amazon River is not affected by the input of lowland tributaries (e.g., Rio Negro) and of Rio Madeira, as there is little variation along the Amazon mainstream. Th concentrations show a bimodal distribution: the Amazon River (Solimões/Ama-

zonas), the Madeira River, and some lowland tributaries (Paraná do Ramos, Arapiuns, and Tapajós) are characterized by low dissolved Th concentrations (8.3–33.4 ng/L), whereas other lowland rivers (Negro, Uatumã, and Trombetas) have high dissolved Th concentrations (83.5–107.6 ng/L). High values are likely to be explained by Th complexation with organic colloids as dissolved Th concentrations are well correlated with dissolved organic carbon (DOC) contents (Fig. 3A; DOC values from Benedetti et al., 2003) and previous studies have shown the importance of organic colloids on Th mobility (Porcelli et al., 2001; Viers et al., 1997). Radium concentrations range from 1.8 (Lago Grande do Curuai outlet) to 49.7 fg/L (Trombetas). Rivers draining the Andes (Amazon, Madeira) show relatively low Ra concentrations (<25 fg/L), whereas lowland tributaries exhibit higher values (>30 fg/L). Previous Ra data on Amazon rivers from Moore and Edmond (1984) show similar systematics. Similar to Th, the mobility of ^{226}Ra seems to be enhanced by the complexation with organic colloids as a good correlation is observed between dissolved ^{226}Ra concentrations and DOC contents (Fig. 3B). The ^{226}Ra concentration for the Amazon River is in the same range as other major rivers but the Th concentration is higher (probably because of the contribution of organic-rich rivers like Rio Negro) and U is lower, probably because of limited carbonate dissolution (Chabaux et al., 2001; Moore, 1967; Palmer and Edmond, 1993; Porcelli et al., 2001; Sarin et al., 1990; Vigier et al., 2001, 2005).

Most (^{234}U/^{238}U) activity ratios in the dissolved load are above 1, which indicates an enrichment of ^{234}U relative to its parent, with values ranging from 0.99 (Negro) to 2.04 (Arapiuns). Rivers draining the Andes show a moderate and relatively constant ^{234}U excess (^{234}U/^{238}U) = 1.23 ± 0.02 ($n = 10$; 2σ), whereas lowland rivers can be divided into two groups: tributaries from the Northern basin show values close to or at secular equilibrium while those from the Southern basin exhibit the highest ^{234}U excess. (^{238}U/^{230}Th) ratios range from 1.79 (Negro) to 17.3 (Solimões). The lowest (^{238}U/^{230}Th) ratios are for lowland rivers (<5) whilst the highest are for rivers draining the Andes (>6). (^{226}Ra/^{230}Th) range from 8.0 (AM6/1-07 LB, Amazonas before Madeira, near left bank) to 19.5 (Solimões). Rivers draining the Andes show a high ^{226}Ra excess, whereas lowland tributaries are characterized by reduced (e.g., Negro) to high ^{226}Ra excess (e.g., Tapajós).

The average (^{234}U/^{238}U) ratio for the Amazon River (1.23 ± 0.02; 2σ, $n = 7$) is within the range of other major rivers but higher than the average riverine ratio (1.17; Chabaux et al., 2001, and refs therein) and the value for the Amazon determined earlier by Moore (1967) (1.10 ± 0.06). (^{238}U/^{230}Th) and (^{226}Ra/^{230}Th) values for the Amazon are low compared to those of other major rivers (Porcelli et al., 2001; Sarin et al., 1990; Vigier et al., 2001, 2005). Relationships between (^{234}U/^{238}U), (^{238}U/^{230}Th), and (^{226}Ra/^{230}Th) ratios and soluble/insoluble element ratios (e.g., Mg/Al, Ca/Ti, and Na/Sm; not shown) indicate that Amazon water characteristics are simply the result of mixing between tributary waters. The poor quality of correlations for (^{234}U/^{238}U) and (^{226}Ra/^{230}Th) ratios reflects the broad range of values in lowland rivers.

(^{230}Th/^{232}Th) ratios range from 0.366 (Trombetas) to 0.721 (AM6/1-12, Amazonas after Parintins). Amazon and Madeira rivers exhibit the highest values. Lowland rivers are characterized by low values, except for Rio Tapajós, whose ratio is comparable to those of rivers draining the Andes. The average value for the Amazon River is 0.66 ± 0.07 (1σ; $n = 8$), which is lower than the upper continental crust value (0.8; calculated using U and Th concentrations taken from Taylor and McLennan, 1985). When compared to those of other major rivers, the (^{230}Th/^{232}Th) value for the Amazon is close to silicate-draining rivers (e.g., Narmada–Tapti; Vigier et al., 2005) whereas rivers draining carbonates have higher values (e.g., Mackenzie; Vigier et al., 2001). When compared to the recent U-series study of the Amazon River by Marques et al. (2003), our U concentrations (^{234}U/^{238}U) and (^{238}U/^{230}Th) ratios, are in good agreement with their results, considering the large error bars in their alpha-counting measurements for activity ratios.

4.2. Suspended particles

Results for suspended particles are given in Table 4. U concentrations in the suspended particles do not show large variations, ranging from 3.03 (Amazonas at Óbidos) to 4.13 ppm (Trombetas). These values are all higher than in the upper crust (2.8 ppm; Taylor and McLennan, 1985), indicating that even if U is mobilized during weathering, it is less so than elements like Ca or Na and ultimately, it is enriched in residues of weathering. Note that, except for the Rio Trombetas, lowland and Andean rivers have similar U concentrations. Th concentrations range from 13.5 (Amazonas before Madeira, near right bank) to 23.2 ppm (Trombetas). All the particles have Th/U ratios higher than an average upper continental crust composition (3.8; Taylor and McLennan, 1985). Suspended sediments exported by the Amazon show U and Th concentrations similar to those of sediments transported by the Mackenzie river (Vigier et al., 2001), but significantly higher than those from the Narmada and Tapti rivers which drain mostly basaltic terranes (Vigier et al., 2005). ^{226}Ra concentrations range from 1.25 (Amazonas before Madeira, near right bank) to 3.65 pg/g (Trombetas). While rivers draining the Andes (Solimões/Amazonas and Madeira) have similar ^{226}Ra concentrations (<1.4 pg/g), lowland rivers show more variable and higher values (>1.8 pg/g). As for uranium, ^{226}Ra concentrations in particles are higher than in the average upper crust (0.958 pg/g; calculated with the U concentration for upper crust from Taylor and McLennan, 1985), showing that Ra is not as mobile as typical soluble elements like Na or Ca, or that its accumulation is controlled by the ^{230}Th budget.

($^{234}U/^{238}U$) ratios in particles are close to secular equilibrium, ranging from 0.979 (Amazonas after Parintins) to 1.033 (Negro) (Fig. 2A). Note that lowland rivers (except for Paraná do Ramos) exhibit ($^{234}U/^{238}U$) > 1, which is surprising as the opposite is generally expected for suspended particles (Vigier et al., 2001). The value for the Amazon River close to its mouth (Amazonas at Óbidos; 0.995 ± 0.011) shows that particles delivered to the ocean are nearly in secular equilibrium. ($^{230}Th/^{238}U$) ratios range from 0.262 (Negro) to 1.50 (Paraná do Ramos) (Fig. 2A). Rio Negro and Rio Trombetas show ^{238}U enrichment relative to ^{230}Th, which is the opposite of what is usually expected for suspended particles. The Amazon River shows variable ($^{230}Th/^{238}U$) ratios, from 1.12 to 1.32. This range is similar to values exhibited by other major rivers (Vigier et al., 2001, 2005). The lowest value corresponds to a sample collected near the left bank of the Rio Amazonas before the confluence with Rio Madeira. It may result from the contribution of Rio Negro particles with ($^{230}Th/^{238}U$) < 1. A simple mass balance calculation suggests that 16% of the particles may have originated from Rio Negro, for the left bank, and only 10%, for the right bank. Considering the mean annual water discharge and sediment fluxes observed for Rio Solimões and Rio Negro (Filizola, 1999), a perfect mixing between the suspended loads of the two tributaries would suggest a contribution for Rio Negro particles of only 7%. The other ($^{230}Th/^{238}U$) values (1.17–1.32) along the Amazon mainstream may result from imperfect mixing between the particles from Rio Solimões (1.27) and Rio Madeira (1.17), the two major suppliers of sediments to the Rio Amazonas. ($^{226}Ra/^{230}Th$) ratios range from 0.86 (Solimões) to 8.3 (Negro) (Fig. 2B). As observed for other ratios, the lowland rivers have unusual characteristics, with ($^{226}Ra/^{230}Th$) higher than 1, whereas ratios lower than 1 are expected in suspended particles. The ($^{226}Ra/^{230}Th$) ratios for the Amazon show a small ^{226}Ra depletion, which is similar to that observed for the Mackenzie River (Vigier et al., 2001). Finally, ($^{230}Th/^{232}Th$) ratios range from 0.177 (Negro) to 0.885 (Solimões), with the lowest values for Negro and Trombetas rivers (Fig. 2C). It is worth noting that, while minor lowland rivers (Uatumã, Paraná do Ramos) generally have characteristics similar to those of Negro and Trombetas rivers, their ($^{230}Th/^{232}Th$) ratios are in the same range as those of Solimões and Madeira rivers. The ($^{230}Th/^{232}Th$) ratio for the Amazon River is close to the ratio for upper continental crust (0.81), and, respectively, lower and higher than measurements of Mackenzie (Vigier et al., 2001) and Deccan river particles (Vigier et al., 2005). Finally, particles show a wider range of ($^{230}Th/^{232}Th$) ratios than that in the dissolved phase, while their ($^{238}U/^{232}Th$) ratios are less variable.

When comparing with the study of Marques et al. (2003), our measurements of Th concentration agree overall with their data, as well as the ($^{234}U/^{238}U$) ratio >1 observed for Rio Negro. However, Marques et al. (2003) observed ($^{234}U/^{238}U$) and ($^{230}Th/^{238}U$) both higher and

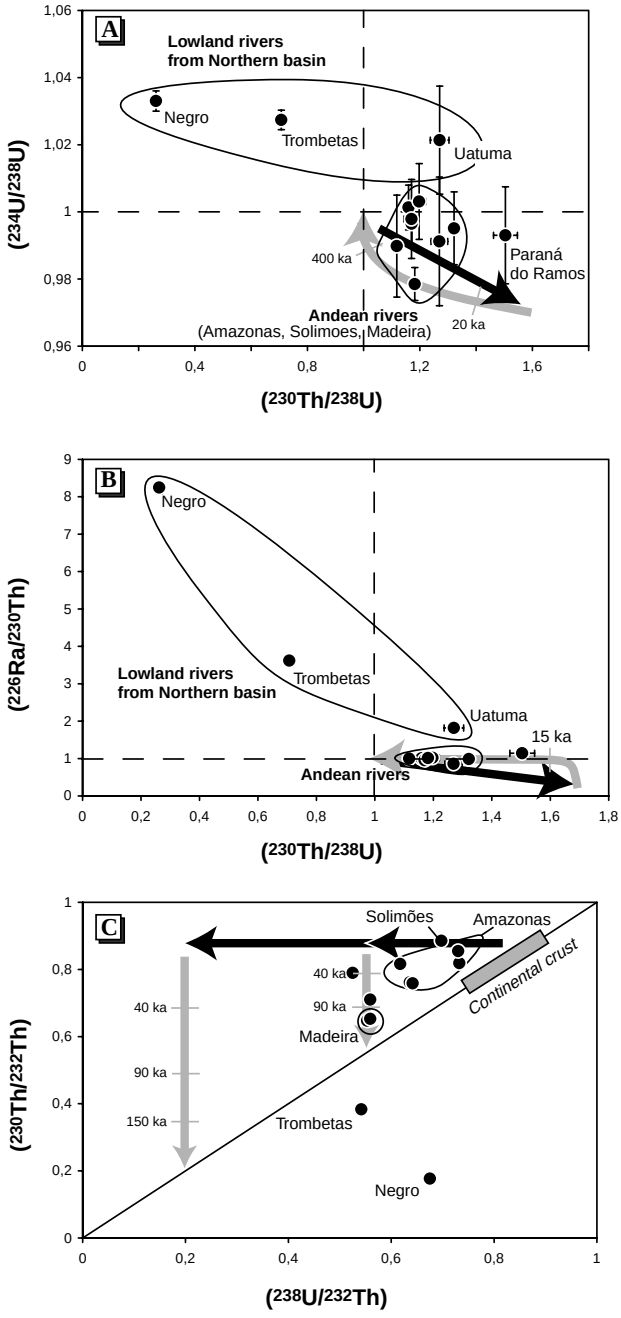

Fig. 2. Daughter–parent activity ratios in suspended particles. (A) ($^{234}U/^{238}U$) and (B) ($^{226}Ra/^{230}Th$) versus ($^{230}Th/^{238}U$), (C) ^{230}Th–^{238}U isochron diagram. Black arrows: weathering-induced fractionation (preferential ^{226}Ra and ^{238}U removal from particles and ^{234}U loss by recoil effect). An instantaneous fractionation is assumed relative to ^{234}U, ^{230}Th, and ^{226}Ra half-lives. The gray arrows show the effect of radioactive decay (return to secular equilibrium) assuming that suspended particles behave as a closed system after fractionation. Some lowland rivers (Trombetas, Negro) exhibit unusual ratios since they are characterized by ($^{230}Th/^{238}U$) < 1, ($^{226}Ra/^{230}Th$), and ($^{234}U/^{238}U$) > 1, where the opposite is expected from weathering. In addition, they show very low ($^{230}Th/^{232}Th$) ratios compared to those of other rivers, which have values close to an average continental crust (shaded area; value inferred from the Th/U of Taylor and McLennan, 1985). In these diagrams (and all the following), parentheses denote activity ratios and error bars, if not shown, are within the symbol size.

lower than 1 for the Rio Solimões/Amazonas, which contrasts with our observations of ratios $\leqslant 1$. Finally, the (^{230}Th/^{238}U) they measured for Rio Negro (1.81 ± 0.22) contrasts with our observation for this river (0.262 ± 0.003).

4.3. Bed sands

Bed sands have been analyzed for Rio Solimões (AM6/1-01), Rio Madeira at Urucurituba (AM6/1-03), and Rio Amazonas at Parintins (AM6/1-10) (Table 5). U concentrations range from 1.24 to 2.86 ppm, Th from 6.31 to 12.25 ppm, and ^{226}Ra from 0.412 to 0.615 pg/g. These abundances are up to three times lower than those in suspended particles and may reflect the differing mineralogy of these materials as bed sands are preferentially enriched in quartz ($SiO_2 = 89\%$ for Madeira). The variations in U, Th, and ^{226}Ra concentrations are probably controlled by the amount of quartz in bed sands, since U, Th, and ^{226}Ra concentrations correlate negatively with the SiO_2 content (not shown). It is worth pointing out that these negative correlations indicate that, for pure silica ($SiO_2 = 100$ wt%), U, Th, and ^{226}Ra concentrations are significantly greater than zero. This is surprising as quartz is not likely to contain substantial amounts of these elements. This most probably reflects the contribution to bed sands of heavy minerals like zircon, which have high U and Th contents (and therefore ^{226}Ra).

^{234}U–^{238}U in bed sands is close to secular equilibrium. (^{230}Th/^{238}U) range from 1.09 to 1.21 and (^{226}Ra/^{230}Th) ratios from 0.80 to 0.92. Thus, ^{230}Th–^{238}U disequilibrium is lower than in suspended particles, except for Madeira, whereas ^{226}Ra deficit is higher. (^{238}U/^{232}Th) and (^{230}Th/^{232}Th) ratios are in the range of suspended particles, but with a lower variability of (^{230}Th/^{232}Th) for bed sands.

5. Discussion

5.1. Weathering in the lowlands: U-series characteristics and their implications

5.1.1. Exchanges between particulate and dissolved loads

Whereas one would expect (^{238}U/^{230}Th), (^{226}Ra/^{230}Th), and (^{234}U/^{238}U) ratios >1 in the dissolved phase and the opposite in particles, some lowland rivers (Negro, Trombetas, and Uatumã) show very different characteristics (Fig. 2): (1) low (^{238}U/^{230}Th) and (^{238}U/^{232}Th) associated with high Th concentrations, in the dissolved load; (2) (^{238}U/^{230}Th) and (^{226}Ra/^{230}Th) > 1 associated with high ^{226}Ra concentrations, in suspended particles. In Section 4.1, we suggested that Th complexation with organic colloids accounts for high concentrations in the dissolved phase. This increase in Th content is also likely to explain the lower (^{238}U/^{230}Th) and (^{238}U/^{232}Th) in the dissolved load. This hypothesis is supported by the negative correlations observed between (^{238}U/^{230}Th), (^{238}U/^{232}Th) ratios and Th as well as DOC contents (Fig. 3; DOC data from Benedetti et al., 2003). Moreover, mass balance calculations show that for these rivers, only 65–75% of the Th transported is in the particulate load (compared to 98–99.9% for Amazon and Madeira rivers). Hence, Th mobilization might also significantly affect activity ratios in suspended particles.

It is possible to quantify the effect of Th mobilization on (^{238}U/^{230}Th) and (^{238}U/^{232}Th) activity ratios in the dissolved and particulate phases by considering a simple mass balance on particles and dissolved phase, before and after removal of particulate Th through complexation with organic colloids. For instance, the mass balance for the (^{238}U/^{232}Th) ratio is written as follows:

$$\left(\frac{^{238}\mathrm{U}}{^{232}\mathrm{Th}}\right)_{\mathrm{d,i}} \cdot \mathrm{Th}_{\mathrm{d,i}} + \mathrm{SM} \cdot \left(\frac{^{238}\mathrm{U}}{^{232}\mathrm{Th}}\right)_{\mathrm{p,i}} \cdot \mathrm{Th}_{\mathrm{p,i}} = \left(\frac{^{238}\mathrm{U}}{^{232}\mathrm{Th}}\right)_{\mathrm{d,f}} \cdot \mathrm{Th}_{\mathrm{d,f}} + \mathrm{SM} \cdot \left(\frac{^{238}\mathrm{U}}{^{232}\mathrm{Th}}\right)_{\mathrm{p,f}} \cdot \mathrm{Th}_{\mathrm{p,f}}, \quad (1)$$

where Th is the Th concentration (ng/L in the dissolved phase, ng/g in the suspended particles), *SM* is the suspended matter content (g/L), the subscripts d and p stand for the dissolved and particulate loads, respectively, and i and f are the initial (before exchange) and final states (after exchange).

Final dissolved and particulate compositions are the observed compositions and the initial dissolved composition is inferred by extrapolating the correlations in Fig. 3 to a DOC content = 0: $\mathrm{Th}_{\mathrm{d,i}} = 10$ ng/L, (^{238}U/^{230}Th)$_{\mathrm{d,i}} = 15$, and (^{238}U/^{232}Th)$_{\mathrm{d,i}} = 11$. Initial composition in the suspended particles is then calculated using mass balance equations. For Rio Negro, it yields: $\mathrm{Th}_{\mathrm{p,i}} = 29.5$ ppm, (^{238}U/^{230}Th)$_{\mathrm{p,i}} = 0.74$, and (^{238}U/^{232}Th)$_{\mathrm{p,i}} = 0.044$. Note that these activity ratios are in the range of those measured for a lateritic soil profile in the Rio Negro basin by Mathieu et al. (1995). Removal of particulate Th can account for Th concentrations, (^{238}U/^{230}Th), (^{238}U/^{232}Th), and (^{230}Th/^{232}Th) ratios in particulate and dissolved loads of Rio Negro by considering that about 50% of the particulate Th has been removed during exchange ($\mathrm{Th}_{\mathrm{p,f}}/\mathrm{Th}_{\mathrm{p,i}} \sim 0.5$).

The same approach can be used to reproduce (^{226}Ra/^{230}Th) ratios but it yields that only 20% of the ^{226}Ra excess can be accounted for by Th removal. The remaining excess is likely to be explained by ^{226}Ra adsorption on particles, as suggested by the high ^{226}Ra concentration in particles observed for Negro, Trombetas, and Utatumã rivers. Adsorption of Ra is expected to occur as organic particles and Fe oxyhydroxides are abundant in these rivers (Allard et al., 2002) and radium is known for its affinity with organic compounds (e.g., Greeman et al., 1990; Sheppard et al., 1980) and Fe oxyhydroxides (e.g., Ames et al., 1983; Porcelli et al., 2001).

Suspended particles of Negro, Trombetas, and Uatumã rivers exhibit (^{234}U/^{238}U) $\geqslant 1$. Similar to radium, U has a high affinity for organic matter particles and Fe oxyhydroxides (e.g., Andersson et al., 1998) and adsorption on particles of dissolved U with (^{234}U/^{238}U) > 1 may explain

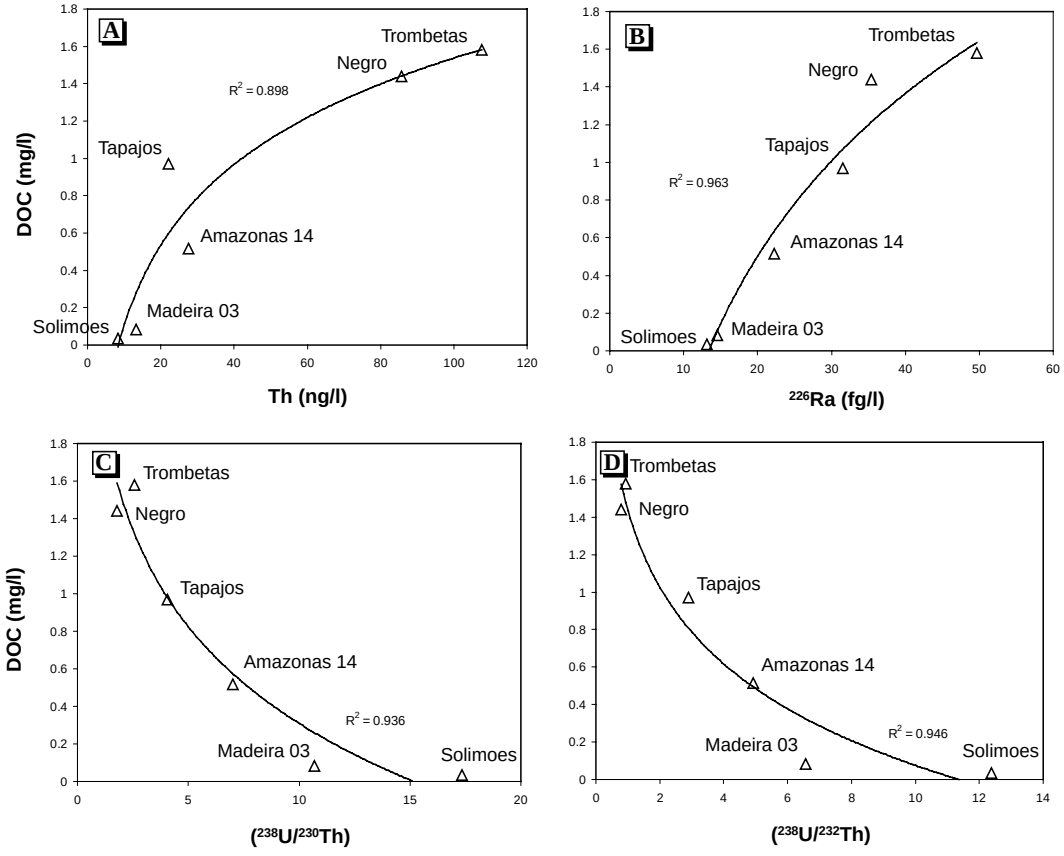

Fig. 3. Dissolved organic carbon (DOC) content versus (A) Th, (B) ^{226}Ra concentrations, (C) (^{238}U/^{230}Th), and (D) (^{238}U/^{232}Th) activity ratios in the dissolved load. Correlation coefficients (R^2) are indicated for logarithmic regression curves. These correlations reflect that, in the dissolved phase, Th, ^{226}Ra concentrations, (^{238}U/^{230}Th) and (^{238}U/^{232}Th) ratios are controlled by the abundance of organic colloids. Regression curves allow us to estimate values for these parameters in the absence of organic matter.

their ^{234}U excess. Mass balance calculations show that, in the lowlands, only 39–49% of the U transported by the river is in the particles (compared to 89–98% for Amazon and Madeira rivers). Consequently, adsorption of dissolved U can significantly affect the U isotope characteristics of particles. Using a mass balance similar to that of the previous paragraph, it is possible to account for U concentrations and (^{234}U/^{238}U) ratios in the particulate and dissolved loads of Rio Negro if we consider that particles have been enriched in U by a factor of 2 and that, before exchange, the dissolved load had a (^{234}U/^{238}U) of ~1.2 (comparable to what is observed in white waters, namely Solimões/Amazonas and Madeira rivers). This process could also potentially account for the low (^{238}U/^{230}Th) and (^{238}U/^{232}Th) ratios in the dissolved phase. Nevertheless, if a combination of particulate Th mobilization, which is required to explain the high Th concentrations in the dissolved load, and U adsorption is considered, quantification of the effect of each process on activity ratios is then difficult to assess.

To summarize, characteristics of particulate and dissolved phases in lowland rivers are explained by the mobilization of particulate Th and the adsorption onto particles of dissolved U and ^{226}Ra. These exchanges can take place in the soil profile (Dequincey et al., 2002) as well as during transport/storage of sediments (e.g., Andersson et al., 1998; Porcelli et al., 2001).

5.1.2. Time scale for erosion in the lowlands

The (^{230}Th/^{232}Th) ratios in suspended particles from Negro and Trombetas rivers are significantly lower than the average value for continental crust, suggesting that they record U–Th fractionation occurring over time scales greater than 75 ka. In order to determine a more precise time scale for weathering in these basins, we used a continuous weathering model similar to that of Vigier et al. (2001) to reproduce their low (^{230}Th/^{232}Th) ratios. This model simulates weathering by continuous removal of elements from the particles. The variation of the abundance of a nuclide, N_i, is written as follows:

$$\frac{dN_i}{dt} = \lambda_{i-1} \cdot N_{i-1} - (\lambda_i + k_i) \cdot N_i, \quad (2)$$

where λ_i and λ_{i-1} are the decay constants of the parent nuclide, N_{i-1}, and the daughter nuclide, N_i, respectively, and k_i is the leaching coefficient of N_i. To calculate the duration of weathering, an estimate of the (^{230}Th/^{232}Th) ratio of the bedrock is required. Pb isotopic composition of suspended

particles can be used for this purpose as Pb isotopic ratios in erosion products will significantly differ from those in the bedrock only if Th–U–Pb fractionation has occurred on time scales greater than 100 Ma. Thus, Pb isotopic composition of the particles reflects those of the bedrock (suspended particle Pb data from Allègre et al., 1996). Inferred Pb isotopic ratios of the bedrock can then be used to estimate its Th/U, by considering a two-stage evolution for Pb isotopes: the first stage corresponds to Pb isotopic evolution in the mantle, and the second follows extraction to the continental crust, at an age estimated from Nd isotopes (see Allègre et al., 1996, for more details on the model). Considering that bedrock is initially in secular equilibrium, its (^{230}Th/^{232}Th) ratio can then be inferred from the Th/U calculated. We obtain for Negro, Trombetas, and Uatumã basins, bedrock (^{230}Th/^{232}Th) ratios equal, respectively, to 0.892, 0.843, and 0.820.

Calculations with the continuous weathering model, using the bedrock (^{230}Th/^{232}Th) ratios estimated in the previous paragraph, yield a duration of weathering (which should be equivalent to the residence time of particles), respectively, of 100, 300, and 500 ka for Uatumã, Trombetas, and Negro river basins (Fig. 4). An alternative model would be to consider a rapid leaching of U (time scale < 10 ka) during a discrete episode of weathering. Following this episode, particles are assumed to behave as a closed system. Estimated particle residence times with this model are 60 ka for Uatumã, and $\geqslant 300$ ka for Negro and Trombetas rivers, which is in the same range as the values calculated with the continuous weathering model. It is also worth pointing out that the time scales inferred for Rio Negro with either of the models are consistent with the study of Mathieu et al. (1995) on a lateritic soil profile in this basin, which suggested that the time needed to create the saprolite was around 300 ka.

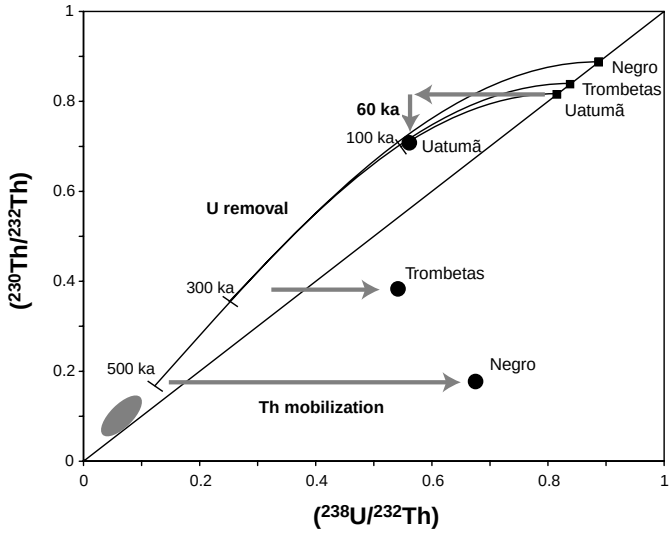

Fig. 4. ^{230}Th–^{238}U isochron diagram for suspended particles of the lowland rivers (dots). Black squares are compositions of the bedrock for each river, inferred from Pb isotopes (see text for details). The gray field represents data for a lateritic soil profile from Rio Negro basin (Mathieu et al., 1995). In the first model, the (^{230}Th/^{232}Th) ratios of Negro, Trombetas, and Utatumã particles can be explained by a continuous U removal over 500, 300, and 100 ka, respectively (solid curves). Parameters used for the calculation are: ^{230}Th leaching coefficient, $k_0 = 4 \times 10^{-7}$ yr^{-1} and ^{238}U leaching coefficient, $k_8 = 4.4 \times 10^{-6}$ yr^{-1}. Alternatively, a rapid leaching of U can be considered (time scale < 10 ka; leftward arrow). Particles operate then as a closed system and ^{230}Th decays (vertical arrow). It yields for the Uatumã river, a residence time of the particles of 60 ka, similar to those obtained by continuous removal. For Negro and Trombetas, this value would be $\geqslant 300$ ka. The ^{238}U excess in Negro and Trombetas particles is explained by Th mobilization (horizontal rightward arrows).

In conclusion, ^{238}U–^{234}U–^{230}Th–^{226}Ra systematics for lowland rivers can be explained by considering the mobilization of particulate Th through complexation with organic colloids, adsorption of dissolved U and ^{226}Ra on suspended particles, and a residence time for particles greater than 100 ka, reflecting their storage in thick soil profiles, with low physical erosion rates (Gaillardet et al., 1997; Guyot, 1993).

5.2. Assessment of the steady-state nature of erosion

A simple model for erosion is to consider that the rate of material exportation as solutes and solids by a river equals the rate of bedrock conversion into soil, over the watershed surface. This is the steady-state model proposed in (Martin and Meybeck, 1979) and tested by Gaillardet et al. (1995) for major and trace elements. It can be written as a simple mass balance equation:

$$M_r = M_w \cdot \mathrm{TDS} + M_p + M_b, \tag{3}$$

where M_r, M_w, M_p, and M_b are, respectively, the masses of bedrock, water, suspended particles, and bedload sands per unit of time. TDS is the total dissolved solid content.

This mass balance can be also written for any chemical element, e.g., for U:

$$U_r \cdot M_r = U_d \cdot M_w + U_p \cdot M_p + U_b \cdot M_b, \tag{4}$$

where U refers to the uranium concentration and the subscripts r, d, p, and b to the bedrock, the dissolved phase, the suspended particles, and the bedload sands, respectively.

This model has been used with U-series in order to establish weathering budgets and determine erosion parameters at a watershed scale, such as erosion rates or sediment yields (Moreira-Nordemann, 1977, 1980; Osmond and Cowart, 1976; Plater et al., 1988, 1994; Porcelli et al., 2001; Vigier et al., 2001). In this case, assuming that erosion operates at steady state on time scales shorter than ^{230}Th half-life, the mass balance for ^{230}Th activity is written as follows:

$$\left(\frac{^{230}\mathrm{Th}}{^{238}\mathrm{U}}\right)_r \cdot U_r \cdot M_r = \left(\frac{^{230}\mathrm{Th}}{^{238}\mathrm{U}}\right)_d \cdot U_d \cdot M_w + \left(\frac{^{230}\mathrm{Th}}{^{238}\mathrm{U}}\right)_p \cdot U_p \cdot M_p + \left(\frac{^{230}\mathrm{Th}}{^{238}\mathrm{U}}\right)_b \cdot U_b \cdot M_b. \tag{5}$$

A similar equation can be written for the other nuclides, ^{234}U, ^{226}Ra, and ^{232}Th, as long as erosion is in steady state

on time scales shorter than the half-life of the nuclide considered. Thus, for ^{234}U–^{238}U, ^{230}Th–^{238}U, and ^{226}Ra–^{238}U systems, it is possible to solve the mass balance equation for the daughter nuclide and determine the amount of suspended matter predicted by a steady-state erosion model and to compare it with the measured values (see Vigier et al., 2001, for more details). For ^{230}Th–^{238}U, we obtain:

$$SM = \frac{U_d \cdot \left[\left(\frac{^{230}Th}{^{238}U}\right)_d - \left(\frac{^{230}Th}{^{238}U}\right)_r\right]}{U_p\left[\left(\frac{^{230}Th}{^{238}U}\right)_r - \left(\frac{^{230}Th}{^{238}U}\right)_p\right] + \frac{M_b}{M_p} \cdot U_b \cdot \left[\left(\frac{^{230}Th}{^{238}U}\right)_r - \left(\frac{^{230}Th}{^{238}U}\right)_b\right]}, \quad (6)$$

where the predicted suspended matter content, SM, is in mg/L, and U_p, and U_b are expressed in ppm and U_d in ng/L.

In this model, it is implicitly assumed that the geochemical characteristics of river material are only derived from weathering. Exchanges between particulate and dissolved phases would perturb these characteristics (see previous section) and rivers, where such processes are significant (e.g., lowland rivers), should not be considered. In contrast, U-series characteristics of rivers draining the Andes in their headwaters (Solimões/Amazonas and Madeira) do not seem to be significantly affected by exchange processes and the dataset for these rivers can be used for testing the steady-state hypothesis. It should be noted that only calculations using the ^{230}Th–^{238}U have yielded meaningful results. The ^{226}Ra–^{238}U system is sensitive to short time scales and the assumptions made above may not be valid. The measurements of $^{234}U/^{238}U$ in particles were not precise enough to allow a good resolution for this calculation.

Results of ^{230}Th–^{238}U calculations are shown for two cases, assuming that the bedrock is initially in secular equilibrium (Table 6 and Fig. 5): (1) the fraction of sediments transported in the river bed is negligible compared to the transport as suspended load ($M_b/M_p \approx 0$), (2) the transport of sediments in the river bed represents 10% of the transport in suspension ($M_b/M_p = 0.1$). In both cases, predicted

Table 6
Comparison between observed and predicted suspended matter

River name	Observed	Predicted ($M_b/M_p = 0$)	Predicted ($M_b/M_p = 0.1$)
Rivers draining the Andes			
Solimões	226	59 ± 2	57 ± 4
Amazone 10	129	69 ± 2	67 ± 3
Amazone 12	177	67 ± 1	
Amazone 14	225	46 ± 1	
Madeira 03	519	47 ± 1	45 ± 2
Madeira 04	443	42 ± 1	
Lowland river			
Uatumã	8	30 ± 1	

Suspended matter contents are expressed in mg/L. Observed values are multi-year averages from (Meade, 1985), except for Amazone 10 where it has been measured during the cruise. Relative uncertainty for observed values is 10%. Predicted values are calculated with a steady-state model using ^{230}Th–^{238}U. The M_b/M_p ratio is the mass fraction of bed load over suspended load.

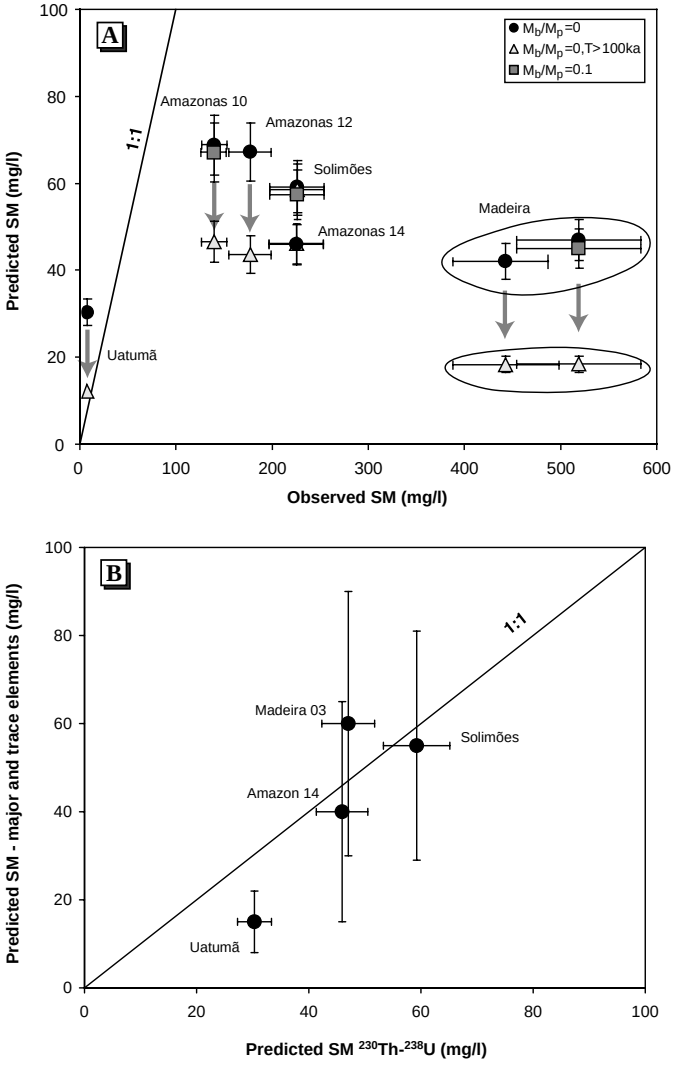

Fig. 5. (A) Predicted suspended matter concentrations by a steady-state erosion model, using ^{230}Th–^{238}U, compared to observed values (multi-year averages from Meade (1985), except for Amazonas 10 where the suspended matter content was measured during the May 2001 sampling cruise). Predicted values are shown considering either that a negligible proportion of sediment is transported in the bedload ($M_b/M_p = 0$; circles), or the amount of sediments transported in the river bed is 10% of the suspended load ($M_b/M_p = 0.1$; squares), or a residence time of suspended particles in the basin is greater than 100 ka and $M_b/M_p = 0$ (triangles). (B) Predicted values for rivers draining the Andes with ^{230}Th–^{238}U are similar to those calculated using major and trace elements (Gaillardet et al., 1997) and lead to the same conclusion, i.e., erosion in the Andes is not in steady state.

SM values are lower than the multi-year averages from Meade (1985). Moreover, if the proportion of bed sands is non-negligible (case 2), the discrepancy between predicted and observed SM values increases.

Four hypotheses can potentially explain the discrepancy between predicted and observed suspended matter contents. The first three hypotheses assume that this discrepancy is due to a poor knowledge of input parameters and erosion is actually in steady state, whereas the last one recognizes the existence of a discrepancy and proposes an explanation for it: (1) suspended particles have a residence

time of the same order of magnitude as (or larger than) ^{230}Th half-life. However, in this case, the ^{230}Th–^{238}U system predicts suspended matter contents to be even lower (Fig. 5A). (2) An alternative explanation would be that the dissolved U concentration used in the calculations is not representative of the mean annual concentration. When evaluating the effect of variations in dissolved U concentration on the predicted suspended matter contents, it turns out that to reconcile observed and predicted suspended matter contents, the dissolved U concentration has to be 100% higher than the measured values. However, Seyler and Boaventura (2003) have shown that U concentration varies little during the year. Consequently, we believe that an improper estimate of the measured dissolved concentrations is unlikely to account for the deviation from steady-state erosion. (3) The contribution of deep groundwaters, which is not directly considered in our calculation, could possibly explain the lower than expected SM values. It is then possible to calculate the relative contribution of groundwaters to the total flow of river water required for the steady-state erosion model to be verified. Assuming a (^{230}Th/^{238}U) ratio in groundwater of $\sim 10^{-3}$ (Banner et al., 1990; Reynolds et al., 2003; Tricca et al., 2001), the required U concentration in groundwaters must be greater than 500 ng/L for a minimal value for X_g of 11% for the Rio Amazonas at Óbidos (values higher are obtained for the Rio Amazonas at the other locations, Rio Solimões and Rio Madeira). Since the water discharge at Óbidos is 225,100 m^3/s, the groundwater discharge would have to be ≈25,000 m^3/s which is substantial. Moreover, the U concentration in groundwaters would have to be at least one order of magnitude higher than that measured in the river water or observed for aquifers (e.g., Luo et al., 2000; Reynolds et al., 2003; Tricca et al., 2001). Consequently, even if the hypothesis of a significant contribution of deep groundwaters cannot be clearly ruled out, on the basis of the required U concentration, it seems unlikely. (4) Finally, the most likely hypothesis seems to be that the discrepancy between observed and predicted suspended matter contents indicates that Amazon (Solimões/Amazonas) and Madeira rivers currently export more sediments than for steady-state erosion.

Interestingly, if $M_b/M_p = 0$, the ^{230}Th–^{238}U system yields values similar to those calculated using major and trace elements (Gaillardet et al., 1997) where the contribution of bed sands was also neglected (Fig. 5B). Gaillardet et al. (1997) have proposed two hypotheses for explaining why their predicted suspended matter contents are lower than observed values: (1) either the present-day physical denudation rate is higher than the rate of soil production, or (2) the composition of the bedrock is not the average continental crust, as estimated in (Taylor and McLennan, 1995), but sedimentary rocks that have lost a fraction of their soluble elements during previous erosion cycles. In the latter case, by considering a bedrock depleted in soluble elements, Gaillardet et al. (1997) were able to reconcile predicted and observed suspended matter contents. When using U-series isotopes, the composition of the bedrock is known because it is older than 1 Ma and therefore in secular equilibrium. Thus, while recycling of sedimentary rocks cannot be precluded (see Section 5.3.2), it cannot account for the deviation from steady state. Thus, U-series show unambiguously that predicted suspended matter contents lower than observed reflect physical denudation rates higher than the soil production rates and that in the Andes, soils are destroyed more rapidly than they are produced. Because Andean soils are thin (e.g., Guyot, 1993), this state cannot have lasted more than 10 ka. This implies a recent change in the conditions of erosion. D'Odorico (2000) showed that, using a deterministic function for soil production and a stochastic approach for physical erosion, the probability distribution of soil thickness is bimodal, with either a thin soil cover or a deep profile, corresponding to the two erosion regimes known as weathering-limited and transport-limited, respectively (e.g., Carson and Kirby, 1972; Stallard and Edmond, 1983). Intermediate thicknesses are unstable and the system evolves from one steady state to another, depending on external forcings such as climate or tectonics. Hence, it is possible that a recent change in the conditions of erosion in the Andes (increase in precipitations, uplift rate, and land use) has induced the transition from a transport-limited regime to a weathering-limited one and accounts for the high denudation rates. In the following, we attempt to constrain the time scale of erosion in the Andes in order to understand when this perturbation might have occurred and how it could relate to climatic, tectonic, and/or anthropic events in this region.

5.3. Time scale and history of erosion for Andean rivers inferred from suspended particles

In the previous section, we inferred that erosion in the Andes is not operating at steady state and suggested that soils are currently being destroyed in response to a recent change in denudation rates. An important corollary is that U-series isotope models which assume that steady state is reached will not be strictly valid. Thus, disequilibria in the particulate and dissolved loads cannot be considered simultaneously to constrain the time scale of erosion. In this section, we use U-series data in suspended particles of Solimões, Amazonas, and Madeira rivers to constrain the duration of chemical weathering in the Andes.

5.3.1. Short time scale for weathering and sediment transfer

The (^{230}Th/^{232}Th) ratios in particles of Rio Solimões/Amazonas are close to the expected value for upper continental crust (≈0.8), inferred with the Th/U ratio from (Taylor and McLennan, 1985) (Fig. 2C). This suggests that: (1) the composition of the bedrock eroded in these basins may be similar to that of pristine, or unweathered, continental crust, (2) Th and U have been fractionated during weathering on short time scales (less than 100 ka).

A continuous weathering model similar to that used by Vigier et al. (2001) can then be used to model the evolution

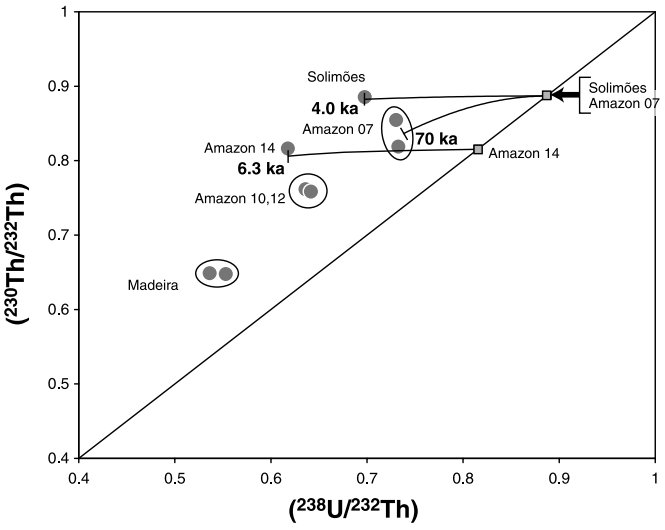

Fig. 6. ^{230}Th–^{238}U isochron diagram for Solimões/Amazonas suspended particles. Curves show continuous weathering, calculated with a model similar to Vigier et al. (2001). Numbers indicate the duration of weathering for particles, equivalent to their residence time in the basin if we assume that they have been continuously weathered since their extraction from the bedrock. Parameters used in the calculations are: (1) the ratio of ^{238}U over ^{230}Th leaching coefficients, k_{238}/k_{230}, taken to be 10 for all rivers which results in a (^{230}Th/^{238}U) ratio in the dissolved phase within the observed range; (2) the leaching coefficient for ^{230}Th is taken to fit the data: $k_{230} = 7 \times 10^{-6}$ yr^{-1} for the Rio Solimões, 3×10^{-7} yr^{-1} for the Rio Amazonas before the confluence with Rio Madeira (Amazonas 07), and 5×10^{-6} yr^{-1} for the Rio Amazonas at Óbidos (Amazonas 14); (3) the bedrock composition (solid squares), inferred from Pb isotopes using a two-stage evolution model (see Section 5.1).

of (^{230}Th/^{232}Th) and (^{238}U/^{232}Th) ratios in the particles of these rivers (see Section 5.1 for a description of the model). The initial composition of the bedrock has been inferred from Pb isotopes assuming a two-stage isotopic evolution (see Section 5.1), since Pb isotopic ratios are not modified by U–Th–Pb fractionation younger than 100 Ma. The results of the calculations (Fig. 6) suggest that the duration of weathering for Rio Solimões (4.0 ± 1 ka) and Rio Amazonas (6.3 ± 1 ka) is indeed short. Nevertheless, the Rio Amazonas before the confluence with Rio Madeira exhibits a higher value (70 ± 2 ka). This might reflect the contribution of particles from Rio Negro, characterized by a large duration of weathering (~500 ka), since at this location, the contribution of Rio Negro to Rio Amazonas is the highest.

5.3.2. Sediment recycling over previous erosion cycles

To investigate the hypothesis of sediment recycling for Andean rivers as suggested by Gaillardet et al. (1999a,b), we have considered Th isotope systematics as a record of U–Th fractionation over time scales greater than ~100 ka. In Fig. 7, (^{230}Th/^{232}Th) ratios in suspended particles are negatively correlated with Sm/Na and Ti/Ca ratios normalized to Upper Continental Crust (UCC) (Taylor and McLennan, 1985). This indicates that there is a strong link between the soluble element depletion in suspended particles (increasing with normalized Sm/Na and Ti/Ca ratios) and Th–U fractionation over time scales greater

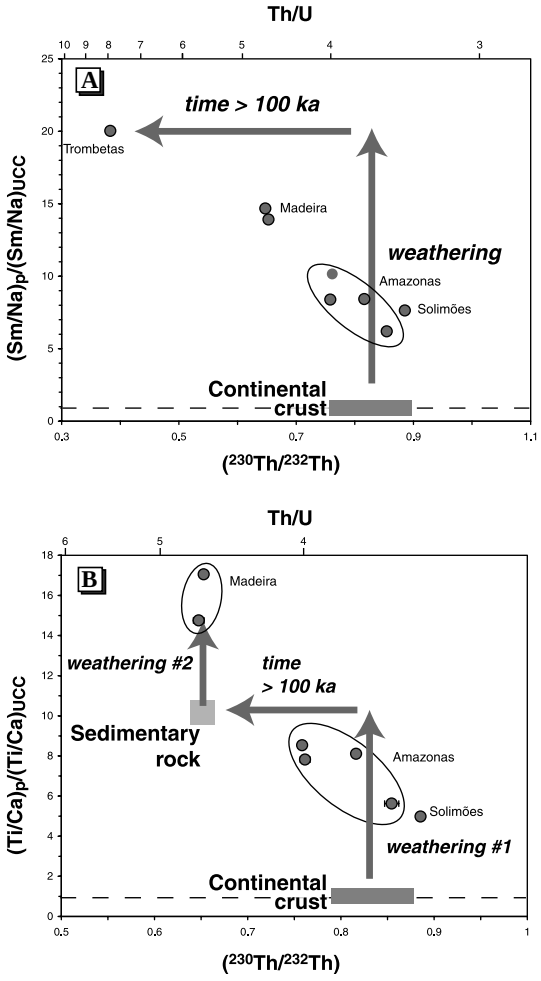

Fig. 7. (A) Sm/Na and (B) Ti/Ca ratios normalized to upper continental crust (UCC) versus (^{230}Th/^{232}Th), in suspended particles. The negative trend suggests a link between soluble element depletion (increasing normalized Sm/Na and Ti/Ca ratios) and the preferential removal of U over Th over time scales >100 ka. Low (^{230}Th/^{232}Th) can be interpreted as the consequence of either (1) weathering of a pristine continental crust over time scales greater than 100 ka, this is the preferred hypothesis for Trombetas river (see Section 5.1); or (2) a multi-step U removal, through several erosion cycles and sediment recycling, as shown by the arrows in (B). Major and trace element data for Trombetas river are taken from Gaillardet et al. (1997).

than 100 ka. This can be explained either by (a) weathering of a pristine continental crust over long time scales or (b) multi-step soluble element removal through several erosion cycles and sediment recycling. For Rio Trombetas, the first hypothesis is more likely for several reasons: (1) this river drains the granodioritic Guyana Shield, hence sediment recycling is unlikely to have occurred in this region because of tectonic stability; (2) as a result of a thick, strongly weathered soil profile, it is more likely that the large soluble element depletion has been produced by severe weathering of silicate rocks of the Guyana Shield (e.g., Almeida et al., 2000) over long periods of time (>100 ka); (3) as shown in Section 5.1, a long time scale of erosion (~300 ka) is required to explain the U-series disequilibria observed in the particulate and dissolved loads of this river.

In the case of the Madeira river, the second hypothesis (b) could be adequate as sedimentary rocks are abundant in the Andean part of the basin (the major source of sediments). In addition, the rocks currently eroded in the outer part of the chain are sediments derived from the destruction of rocks located in the inner part, and that have now been integrated to the Cordillera as a consequence of crustal shortening. In Dosseto (2003), the duration of weathering is estimated for the different regions of the Rio Madeira basin (Andes, foreland basin and tropical plain) by modeling the ^{238}U–^{230}Th–^{226}Ra disequilibria observed in suspended particles using a continuous weathering model. The time scale of weathering for the Rio Madeira at the confluence with the Rio Amazonas is 19 ± 6 ka. This value and the leaching coefficients used in the calculation can then be used to draw the corresponding curve for continuous weathering of particles on the ^{230}Th–^{238}U isochron diagram (Fig. 8A). It appears that the resulting ($^{238}U/^{232}Th$) for the bedrock (0.66) is significantly lower than those of a pristine continental crust (0.8). This means that the bedrock must have lost part of its uranium more than 300 ka ago, which supports the hypothesis of sediment recycling for explaining the low ($^{230}Th/^{232}Th$) in particles of Rio Madeira. This hypothesis is further investigated based on a combination of Pb and Th isotopes in what follows.

If the bedrock has lost uranium more than 100 Ma ago, it may have affected its Pb isotopic ratios of particles com-

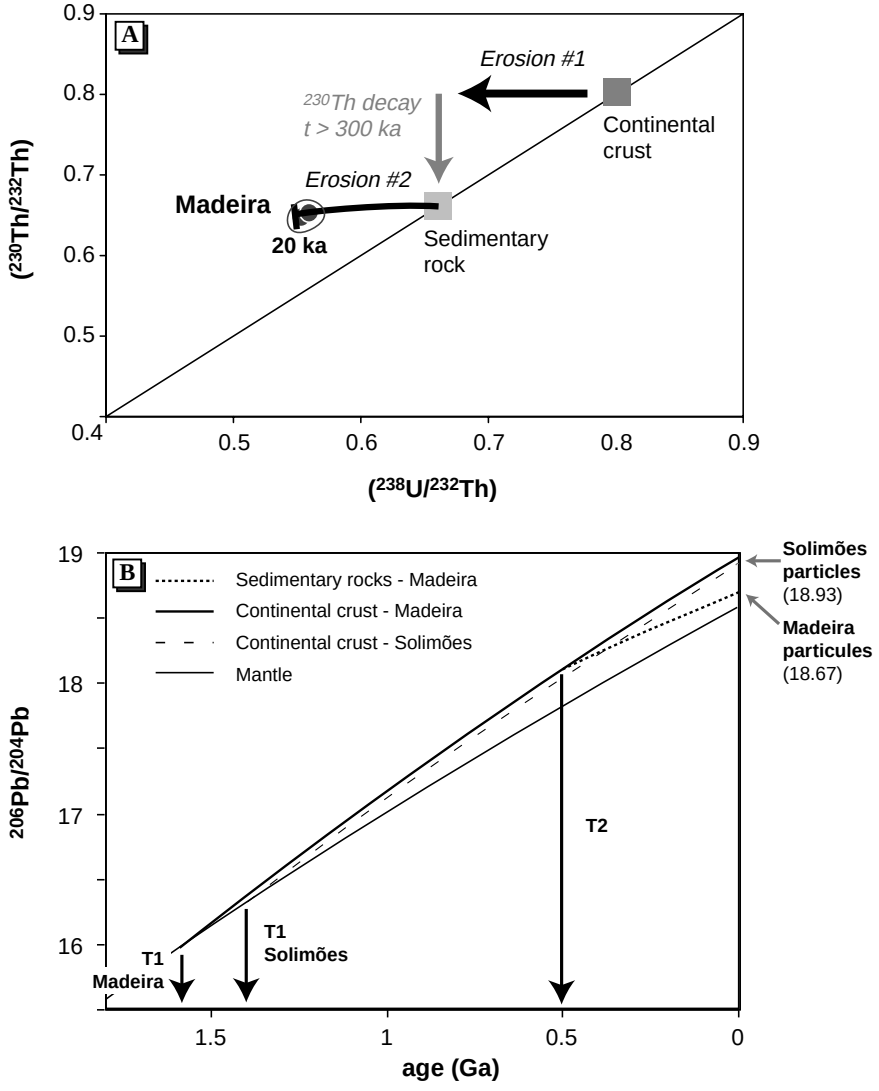

Fig. 8. (A) ^{230}Th–^{238}U isochron diagram for Madeira suspended particles. The curve is calculated to reproduce the composition of particles using parameters from Dosseto (2003) for a continuous weathering model. The inferred ($^{230}Th/^{232}Th$) for the bedrock is 0.660 ± 5. (B) Evolution of the $^{206}Pb/^{204}Pb$ ratio of particles following a multi-stage model: two stages for Rio Solimões, three for Rio Madeira (see text for details). T_1 is the age of continental crust extraction and T_2 of sedimentary rock production (ancient erosion event). In the case of Rio Madeira, U and Pb are fractionated at T_2 and $^{206}Pb/^{204}Pb$ evolves with a U/Pb lower than that of the crust (dotted line). Calculations show that present-day Pb isotopic ratios after the third stage (evolution in the sediment) can reproduce those in Madeira particles with an age for the ancient erosion event of 500 ± 120 Ma. This is consistent with the age of sedimentary rocks found in the Andean part of the Madeira basin.

pared to a typical crust composition. To further test this hypothesis, the Pb isotopic composition of particles has been modeled using a three-stage evolution (Fig. 8B), assuming that they were extracted from the bedrock less than 100 Ma ago, such that Pb isotopic ratios reflect those of the bedrock (Pb isotope data of particles from Allègre et al., 1996). This is likely to be the case since we have inferred a maximum age for the production of particles of ~20 ka. The two first stages are evolution in the mantle and the continental crust (see Section 5.1) and the third corresponds to evolution in a sedimentary rock, produced by erosion of the crust at a time T_2. At T_2, the crust loses U relative to Pb and Th, which are assumed as perfectly immobile, and the U/Pb and Th/U ratios are accordingly modified. The equations used to calculate the Pb isotopic ratios in particles are as follows:

$$\frac{^{206}Pb}{^{204}Pb} = \alpha_0 + \mu_1 \cdot (e^{\lambda_{238} \cdot T_0} - e^{\lambda_{238} \cdot T_1}) + \mu_2 \cdot (e^{\lambda_{238} \cdot T_1} - e^{\lambda_{238} \cdot T_2}) + \mu_3 \cdot (e^{\lambda_{238} \cdot T_2} - 1), \quad (7)$$

$$\frac{^{207}Pb}{^{204}Pb} = \beta_0 + \frac{\mu_1}{137.88} \cdot (e^{\lambda_{235} \cdot T_0} - e^{\lambda_{235} \cdot T_1}) + \frac{\mu_2}{137.88} \cdot (e^{\lambda_{235} \cdot T_1} - e^{\lambda_{235} \cdot T_2}) + \frac{\mu_3}{137.88} \cdot (e^{\lambda_{235} \cdot T_2} - 1), \quad (8)$$

$$\frac{^{208}Pb}{^{204}Pb} = \gamma_0 + \kappa_1 \cdot \mu_1 \cdot (e^{\lambda_{232} \cdot T_0} - e^{\lambda_{232} \cdot T_1}) + \kappa_2 \cdot \mu_2 \cdot (e^{\lambda_{232} \cdot T_1} - e^{\lambda_{232} \cdot T_2}) + \kappa_3 \cdot \mu_3 \cdot (e^{\lambda_{232} \cdot T_2} - 1), \quad (9)$$

where T_0 is the age of the Earth and T_1, the age for continental crust extraction in the Madeira basin, based on Nd isotope data, is 1.59 Ga (Allègre et al., 1996). λ_{238}, λ_{235}, and λ_{232} are the decay constants of ^{238}U, ^{235}U, and ^{232}Th, respectively. α_0, β_0, and γ_0 are the bulk Earth initial $^{206}Pb/^{204}Pb$, $^{207}Pb/^{204}Pb$, and $^{208}Pb/^{204}Pb$ ratios, respectively. $\alpha_0 = 9.307$, $\beta_0 = 10.294$, and $\gamma_0 = 29.476$ (Tatsumoto et al., 1973). μ_1, μ_2, and μ_3 are the $^{238}U/^{204}Pb$ ratios, and κ_1, κ_2, and κ_3, the $^{232}Th/^{238}U$ ratios in the mantle, the continental crust, and the sedimentary rock, respectively. κ_1 is taken to be 4.15 (Allègre et al., 1986) and $\mu_1 = 9.35$ (Allègre et al., 1996).

In the previous section, it has been shown that, in the Rio Solimões basin, the bedrock has a Th–U composition similar to the average continental crust of Taylor and McLennan (1985) and erosion produces sediments on time scales of a few ka. Consequently, Pb isotopic ratios in suspended particles reflect those of the bedrock and a two-stage model can describe their evolution, similar to lowland rivers (see Section 5.1). Using this model, Allègre et al. (1996) calculated a $^{238}U/^{204}Pb$ for the crust (μ_2) in the Rio Solimões basin of 10.7 and a $^{232}Th/^{238}U$ (κ_2) of 3.4. As the Solimões and Madeira particles have similar $^{208}Pb/^{204}Pb$ (38.85 ± 5 and 38.84 ± 5, respectively) and because Th and Pb are believed to be relatively immobile during weathering, crustal protoliths for both basins must have evolved with similar Th/Pb ratios. It is then reasonable to assume that the continental crust of Rio Madeira basin also had $^{238}U/^{204}Pb$ ($\mu_2 = 10.7$) and $^{232}Th/^{238}U$ ($\kappa_2 = 3.4$) ratios similar to those of Rio Solimões, since these elements do not fractionate greatly during continental crust genesis. The $^{232}Th/^{238}U$ of the sedimentary rock is inferred from Fig. 8A ($\kappa_3 = 4.7$), and because of the relative immobility of Th and Pb during weathering, the $^{232}Th/^{204}Pb$ ratio of particles is similar to the one of the source sedimentary rock and can then be combined with κ_3 to calculate the $^{238}U/^{204}Pb$ of the sedimentary rock ($\mu_3 = 7.3$).

Using these parameters (Table 7), the age of a first erosion cycle, T_2, can be estimated and compared to the age of sedimentary rocks currently eroded in the Madeira basin. We determined the values of T_2 that fit the observed $^{206}Pb/^{204}Pb$, $^{207}Pb/^{204}Pb$, and $^{208}Pb/^{204}Pb$ ratios in suspended particles of the Madeira river (Fig. 8B). Remarkably, this yields an age for the ancient erosion event of 500 ± 120 Ma, which matches the age of the sedimentary rocks eroded in the upper part of the Madeira basin (Guyot, 1993). Consequently, Pb isotope systematics of Rio Madeira can be explained by U–Pb and U–Th fractionation at the time the sedimentary rocks were deposited in the foreland basin. At lower elevations, Cenozoic sedimentary rocks resulting from the erosion of the Paleozoic rocks can also be found but there, the weathering-induced fractionation is too recent to have modified Pb isotopes.

In conclusion, the combination of U-series and Pb isotopes can be used to address the history of erosion in a basin on time scales up to several 100 Ma and the involvement of sediment recycling. More specifically, we show here that the rocks of the Rio Madeira basin were already depleted in mobile elements, which confirms the suggestion of Gaillardet et al. (1999a) that the composition of suspended particles records chemical weathering over the whole erosion history of the basin, including recycling of sedimentary rocks. In contrast, in the Solimões basin, U-series and Pb isotopes are consistent with the erosion of a more pristine crust.

5.3.3. Rapid response of erosion to external forcing

In the preceding sections, we argued that the Rio Solimões/Amazonas and Rio Madeira are characterized by short time scales for chemical weathering (4–20 ka). Moreover, in Dosseto (2003), the time scale of weathering for the Andean part of the Rio Madeira basin is inferred to be similar to that for the Rio Solimões (a few ka). This implies that the suspended particles that do get transported are not stored for long periods in the Andean foreland

Table 7
Parameters used in the Pb isotopic evolution models

	μ_1	κ_1	T_1	μ_2	κ_2	T_2	μ_3	κ_3
Solimões	9.33	4.15	1.41	10.7	3.4		—	—
Madeira (2 stages)	9.35	4.15	1.59	9.6	3.8			
Madeira (3 stages)	9.33	4.15	1.59	10.7	3.4	0.50	7.3	4.7

basin and the tropical plain. Moreover, it has been suggested in Section 5.2 that erosion in the Andes is not in steady state and that soil export rates are faster than soil production. Hence, a perturbation of the erosion regime in the Andes must have occurred in the recent past (1–10 ka). The origin of this recent perturbation may be tectonic, climatic, anthropic or a combination of the three. An increase in the uplift rate of the Andes would induce an increase in the denudation rate, but the time resolution for determining changes in the uplift rate of the Andes is greater than 1 Ma (e.g., Delfaud et al., 1999; Gregory-Wodzicki, 2000). Several recent studies have suggested that precipitation in the Bolivian Andes has been changing during the Holocene (Rigsby et al., 2003; Servant and Servant-Vildary, 2003; Tapia et al., 2003). Following drier conditions during the Early and Middle Holocene, precipitation increased at the beginning of Late Holocene (~4 ka). This may explain why more sediments are currently being exported than what is predicted by a steady-state erosion model and provides an explanation for the recent perturbation in the erosional regime. This conclusion is in agreement with the theoretical work of Whipple (2001), who suggested that, on the one hand, the time scale of a tectonic perturbation may be long compared to the response time of erosion, so that steady-state erosion can be achieved, and on the other hand, rapid climatic fluctuations in the Quaternary may preclude the attainment of steady-state erosion over time scales of tens of ka.

6. Conclusions

The study of the Amazon basin with U-series represents an excellent test for this tool, since it is the largest basin in the world and it is characterized by very diverse weathering regimes, representing a summary of the numerous weathering regimes that can be found around the world. In this study, it has been demonstrated that U-series are tracers of weathering: (1) we have observed very distinct U-series disequilibria in dissolved and particulate phases between the Andes and the tropical plain, (2) U-series disequilibria are closely related to the composition in major and trace elements, and (3) they indicate that suspended particles record weathering over the whole erosion history of the basin, whereas the composition of the dissolved load is only sensitive to present-day weathering.

In shield areas and the tropical plain, the residence time of particles (storage in soil profiles and transport) is greater than 100 ka. In addition, particulate and dissolved loads for these rivers show distinctive characteristics that can be explained by exchange between the two phases during storage of particles in the soil profile and/or transport in the river. During these exchanges, particulate Th would be mobilized because of complexation with organic colloids, and dissolved U and ^{226}Ra may be adsorbed onto the particles.

When using U-series to evaluate if erosion is in steady state, there is no requirement to know the bedrock composition. Hence, it is possible to show unambiguously that present-day denudation rates for basins draining the Andes (Madeira, Solimões/Amazonas) are higher than those predicted by a steady-state erosion model and indicate that soils are currently being destroyed more rapidly than they are produced.

In addition, suspended sediments must have very short residence time in the basins draining the Andes, compared with the lowlands. Using a continuous weathering model similar to Vigier et al. (2001), we calculate 4.0 ± 1 ka for the Rio Solimões and 6.3 ± 1 ka for the Rio Amazonas at Óbidos. These short time scales for weathering, related to the high present-day denudation rates, indicate that a recent perturbation has initiated the destruction of soils in the Andes. The increase in precipitation rates ~4 ka ago in the Bolivian Andes, suggested by recent palaeoclimatic studies, may be an explanation. Consequently, erosion in the Andes seems to rapidly respond to high-frequency climatic fluctuations, which precludes the attainment of steady state.

Finally, by coupling U-series and Pb isotopes in suspended particles, it is possible to track the erosion history in the Rio Madeira basin. We show that, in this basin, erosion is believed to occur as a multi-step process and data can be explained by erosion of a pristine crust 500 ± 120 Ma ago and recycling of sedimentary rocks into the current erosion cycle. The age of the first erosion cycle is consistent with the age of the sediment deposition found in the Andean part of the Madeira basin.

Acknowledgments

We thank Daniel Nahon and the CIRAD (Centre de coopération Internationale en Recherche Agronomique pour le Développement) for funding the field work. Jean-Loup Guyot is thanked as head of the Hybam project (Hydrology of the Amazon basin) for considerable help during field trips and for helpful discussions. We are also grateful to Louise Thomas, Peter Van Calsteren, and Nathalie Vigier for their assistance on the ICP-MS at the Open University, UK, and to Kevin Burton for welcoming us in his department at the Open University. Caroline Gorge is acknowledged for major element analysis and field work, and Michel Valladon (LMTG, Université Paul Sabatier, Toulouse) for trace element measurements. We also thank Laurence Maurice-Bourgoin, Pascal Kosuth, Marc Benedetti, Patrick Seyler, and François Métivier for helpful discussions as well as Simon Turner for helpful remarks on the manuscript. Finally, the three reviewers of the manuscript (an anonymous reviewer, F. Chabaux, and D. Porcelli) as well as the associate editor (S. Krishnaswami) are also greatly thanked for their comments. This work was supported by the INSU PNSE program.

Associate editor: S. Krishnaswami

References

Allard, T., Ponthieu, M., Weber, T., Filizola, N., Guyot, J.-L., Benedetti, M., 2002. Nature and properties of suspended solids in the Amazon Basin. *Bull. Soc. Géol. France* **173** (1), 67–75.

Allègre, C.J., Dupré, B., Lewin, E., 1986. Thorium/uranium ratio of the earth. *Chem. Geol.* **59**, 219–227.

Allègre, C.J., Dupré, B., Négrel, P., Gaillardet, J., 1996. Sr–Nd–Pb isotope systematics in Amazon and Congo River systems: constraints about erosion processes. *Chem. Geol.* **131**, 93–112.

Almeida, F.F.M.d., Neves, B.B.d.B., Carneiro, C.D.R., 2000. The origin and evolution of the South American Platform. *Earth Sci. Rev.* **50**, 77–111.

Ames, L.L., McGarrah, J.E., Walker, B.A., 1983. Sorption of trace constituents from aqueous solutions onto secondary minerals II Radium. *Clays Clay Miner.* **31**, 335–342.

Andersson, P.S., Porcelli, D., Wasserburg, G.J., Ingri, J., 1998. Particle transport of ^{234}U–^{238}U in the Kalix River and the Baltic Sea. *Geochim. Cosmochim. Acta* **62** (3), 385–392.

Banner, J.L., Wasserburg, G.J., Chen, J.H., Moore, C.H., 1990. ^{234}U–^{238}U–^{230}Th–^{232}Th systematics in saline groundwaters from central Missouri. *Earth Planet. Sci. Lett.* **101**, 296–312.

Benedetti, M.F., Mounier, S., Filizola, N., Benaim, J., Seyler, P., 2003. Carbon and metal concentrations, size distributions and fluxes in major rivers of the Amazon basin. *Hydrol. Process.* **17** (7), 1363–1377.

Borole, D.V., Krishnaswami, S., Somayajulu, B.L.K., 1982. Uranium isotopes in rivers, estuaries and adjacent coastal sediments of western India: their weathering, transport and oceanic budget. *Geochim. Cosmochim. Acta* **46** (2), 125–137.

Carson, M.A., Kirby, M.J., 1972. *Hillslope, Form and Process*. Cambridge University Press, Cambridge, MA.

Chabaux, F., Riotte, J., Clauer, N., France-Lanord, C., 2001. Isotopic tracing of the dissolved U fluxes of Himalayan rivers: implications for present and past U budgets of the Ganges–Brahmaputra system. *Geochim. Cosmochim. Acta* **65** (19), 3201–3217.

Chabaux, F., Riotte, J., Dequincey, O., 2003. U–Th–Ra fractionation during weathering and river transport. In: Bourdon, B., Henderson, G.M., Lundstrom, C.C., Turner, S.P. (Eds.), *Uranium-series Geochemistry*, vol. 52. Geochemical Society–Mineralogical Society of America, pp. 533–576.

Cheng, H., Edwards, R.L., Hoff, J., Gallup, C.D., Richards, D.A., Asmerom, Y., 2000. The half-lives of uranium-234 and thorium-230. *Chem. Geol.* **169** (1-2), 17–33.

Claude-Ivanaj, C., 1997. Systématique ^{238}U–^{230}Th–^{226}Ra appliquée au volcanisme actif océanique: contraintes sur la durée et les processus de formation des magmas. PhD thesis, Université Paris 7.

Claude-Ivanaj, C., Bourdon, B., Allegre, C.J., 1998. Ra–Th–Sr isotope systematics in Grande Comore Island: a case study of plume–lithosphere interaction. *Earth Planet. Sci. Lett.* **164** (1–2), 99–117.

Delfaud, J., Sabrier, R., Baudino, R., Lavenu, A., Marocco, R., 1999. Reconstitution des étapes de la surrection des Andes d'Equateur á partir de l'interpretation des mineraux argileux contenus dans les bassins intramontagneux (Miocene á actuel). Reconstruction of Andean uplift stages from clay mineral studies in intramontane basins of Ecuador (Miocene to present). *Bull. Soc. Geol. France* **70** (1), 13–23.

Dequincey, O., Chabaux, F., Clauer, N., Sigmarsson, O., Liewig, N., Leprun, J.-C., 2002. Chemical mobilizations in laterites: evidence from trace elements and ^{238}U–^{234}U–^{230}Th disequilibria. *Geochim. Cosmochim. Acta* **66** (7), 1197–1210.

D'Odorico, P., 2000. A possible bistable evolution of soil thickness. *J. Geophys. Res.* **105** (B11), 927–935.

Dosseto, A., 2003. Étude du magmatisme aux zones de subduction et de l'érosion continentale par les séries de l'Uranium: constraintes sur les processus et leurs temps caractéristique. PhD, Université Paris VII, Denis Diderot.

Filizola Jr., N.P., 1999. O fluxo de sedimentos em suspensão nos rios da bacia amazônica brasileira, pp. 66. ANEEL-Agência Nacional de Energia Elétrica.

Gaillardet, J., Dupre, B., Allègre, C.J., 1999a. Geochemistry of large river suspended sediments: silicate weathering or recycling tracer? *Geochim. Cosmochim. Acta* **63** (23/24), 4037–4051.

Gaillardet, J., Dupré, B., Louvat, P., Allègre, C.J., 1999b. Global silicate weathering and CO_2 consumption rates deduced from the chemistry of large rivers. *Chem. Geol.* **159** (1–4), 3–30.

Gaillardet, J., Dupré, B., Allègre, C.J., 1995. A global mass budget applied to the Congo Basin rivers: erosion rates and continental crust composition. *Geochim. Cosmochim. Acta* **59** (7), 3469–3485.

Gaillardet, J., Dupré, B., Allègre, C.J., Négrel, P., 1997. Chemical and physical denudation in the Amazon River Basin. *Chem. Geol.* **142**, 141–173.

Greeman, D.J., Rose, A.W., Jester, W.A., 1990. Form and behaviour of radium, uranium, and thorium in central Pennsylvania soils derived from dolomite. *Geophys. Res. Lett.* **17** (6), 833–836.

Gregory-Wodzicki, K.M., 2000. Uplift history of the Central and Northern Andes: a review. *Geol. Soc. Am. Bull.* **112** (7), 1091–1105.

Guyot, J.-L., 1993. Hydrogéochimie des fleuves de l'Amazonie bolivienne, ORSTOM.

Langmuir, D., 1978. Uranium solution–mineral equilibria at low temperatures with applications to sedimentart ore deposits. *Geochim. Cosmochim. Acta* **42**, 547–569.

Langmuir, D., Herman, J.S., 1980. The mobility of thorium in natural waters at low temperatures. *Geochim. Cosmochim. Acta* **44**, 1753–1766.

Langmuir, D., Riese, A., 1985. The thermodynamics properties of Ra. *Geochim. Cosmochim. Acta* **49**, 1593–1601.

Luo, S., Ku, T.-L., Roback, R., Murrell, M., McLing, T.L., 2000. In-situ radionuclide transport and preferential groundwater flows at INEEL (Idaho): decay-series disequilibrium studies. *Geochim. Cosmochim. Acta* **64** (5), 867–881.

Manhès, G., 1981. Developpement de l'ensemble chronomètrique U–Th–Pb: contribution à la chronologie initiale du système solaire. Thèse d'état, Université Paris 6.

Marques Jr., A.N., Al-Gharib, I., Bernat, M., Fernex, F., 2003. Uranium and thorium isotopes in the rivers of the Amazonian basin: hydrology and weathering processes. *Hydrol. Process.* **17**, 17–31.

Martin, J.M., Meybeck, M., 1979. Element mass-balance of material carried by major world rivers. *Mar. Chem.* **7**, 173–206.

Mathieu, D., Bernat, M., Nahon, D., 1995. Short-lived U and Th isotope distribution in a tropical laterite derived from granite (Pitinga river basin, Amazonia, Brazil): application to assessment of weathering rate. *Earth Planet. Sci. Lett.* **136**, 703–714.

Meade, R.H., 1985. Suspended sediment in the Amazon river and its tributaries in Brazil during 1982–1984. *U.S. Geol. Surv. Open-File Rep.* **85** (492), 1–40.

Milliman, J.D., Meade, R.H., 1983. World-wide delivery of river sediments to the oceans. *J. Geol.* **1**, 1–21.

Molinier, M., Guyot, J.-L., de Oliveira, E., Guimarães, V., 1995. Les régimes hydrologiques du bassin amazonien. In: L'hydrologie tropicale.

Moore, W.S., 1967. Amazon and Mississippi river concentrations of uranium, thorium, and radium isotopes. *Earth Planet. Sci. Lett.* **2**, 231–234.

Moore, W.S., Edmond, J.M., 1984. Radium and barium in the Amazon River system. *J. Geophys. Res.* **89** (C2), 2061–2065.

Moreira-Nordemann, L.M., 1977. Etude de la vitesse d'altération des roches au moyen de l'uranium utilisé comme traceur naturel. Application à deux bassins du Nord Est du Brésil. PhD, Université Paris VI.

Moreira-Nordemann, L.M., 1980. Use of $^{234}U/^{238}U$ disequilibrium in measuring chemical weathering rate of rocks. *Geochim. Cosmochim. Acta* **44**, 103–108.

Osmond, J.K., Cowart, J.B., 1976. The theory and uses of natural uranium isotopic variations in hydrology. *Atom. Energy Rev.* **14**, 621–679.

Osmond, J.K., Cowart, J.B., 1982. Groundwater. In: Ivanovich, M., Harmon, R.S. (Eds.), *Uranium Series Disequilibrium: Applications to Environmental Problems in Earth Sciences*. Oxford University Press, Oxford, pp. 202–245.

Osmond, J.K., Ivanovich, M., 1992. Uranium-series mobilization and surface hydrology. In: Ivanovich, M., Harmon, R.S. (Eds.), *Uranium-series Disequilibrium: Application to Earth, Marine, and Environmental Sciences*. Oxford Sciences Publications, pp. 259–289.

Palmer, M.R., Edmond, J.M., 1993. Uranium in river water. *Geochim. Cosmochim. Acta* **57**, 4947–4955.

Pande, K., Sarin, M.M., Trivedi, J.R., Krishnaswami, S., Sharma, K.K., 1994. The Indus river system (India–Pakistan): major-ion chemistry, uranium and strontium isotopes. *Chem. Geol.* **116**, 245–259.

Peate, D.W., Hawkesworth, C.J., van Calsteren, P.W., Taylor, R.N., Murton, B.J., 2001. ^{238}U–^{230}Th constraints on mantle upwelling and plume-ridge interaction along the Reykjanes Ridge. *Earth Planet. Sci. Lett.* **187** (3–4), 259–272.

Plater, A.J., Dugdale, R.E., Ivanovich, M., 1988. The application of uranium series disequilibrium concepts to sediment yield determination. *Earth Surf. Proc. Landforms* **13**, 171–182.

Plater, A.J., Dugdale, R.E., Ivanovich, M., 1994. Sediment yield determination using uranium-series radionuclides: the case of The Wash and Fenland drainage basin, eastern England. *Geomorphology* **11** (1), 41–56.

Plater, A.J., Ivanovich, M., Dugdale, R.E., 1992. Uranium series disequilibrium in river sediments and waters: the significance of anomalous activity ratios. *Appl. Geochem.* **7**, 101–110.

Porcelli, D., Andersson, P.S., Baskaran, M., Wasserburg, G.J., 2001. Transport of U- and Th-series nuclides in a Baltic Shield watershed and the Baltic Sea. *Geochim. Cosmochim. Acta* **65** (15), 2439–2459.

Porcelli, D., Andersson, P.S., Wasserburg, G.J., Ingri, J., Baskaran, M., 1997. The importance of colloids and mires for the transport of uranium isotopes through the Kalix River watershed and Baltic Sea. *Geochim. Cosmochim. Acta* **61** (19), 4095–4113.

Reynolds, B.C., Wasserburg, G.J., Baskaran, M., 2003. The transport of U- and Th-series nuclides in sandy confined aquifers. *Geochim. Cosmochim. Acta* **67** (11), 1955–1972.

Rigsby, C.A., Baker, P.A., Aldenderfer, M.S., 2003. Fluvial history of the Rio Ilave valley, Peru, and its relationship to climate and human history. *Palaeogeogr. Palaeoclimatol. Palaeoecol.* **194** (1–3), 165–185.

Riotte, J., Chabaux, F., 1999. ($^{234}U/^{238}U$) activity ratios in freshwaters as tracers of hydrological processes: the Strengbach watershed (Vosges, France). *Geochim. Cosmochim. Acta* **63** (9), 1263–1275.

Riotte, J., Chabaux, F., Benedetti, M., Dia, A., Gérard, M., Boulègue, J., Etamé, J., 2003. U colloidal transport and origin of the ^{234}U–^{238}U fractionation in surface waters: new insights from Mount Cameroon. *Chem. Geol.* **202** (3–4), 365–381.

Sarin, M.M., Krishnaswami, S., Somayajulu, B.L.K., Moore, W.S., 1990. Chemistry of uranium, thorium, and radium isotopes in the Ganga–Brahmaputra river system: weathering processes and fluxes to the Bay of Bengal. *Geochim. Cosmochim. Acta* **54**, 1387–1396.

Servant, M., Servant-Vildary, S., 2003. Holocene precipitation and atmospheric changes inferred from river paleowetlands in the Bolivian Andes. *Palaeogeogr. Palaeoclimatol. Palaeoecol.* **194** (1–3), 187–206.

Seyler, P., Boaventura, G., 2003. Distribution and partition of trace metals in the Amazon basin. *Hydrol. Process.* **17** (7), 1345–1362.

Sheppard, J.C., Campbell, M.J., Cheng, T., Kittrick, J.A., 1980. Retention of radionuclides by mobile humic compounds and soil particles. *Environ. Sci. Technol.* **14**, 1349–1353.

Sioli, H., 1968. Hydrochemistry and geology in the Brazilian Amazon region. *Amazoniana* **1**, 267–277.

Stallard, R.F., Edmond, J.M., 1983. Geochemistry of the Amazon, 2. The influence of geology and weathering environment on the dissolved load. *J. Geophys. Res.* **88** (C14), 9671–9688.

Tapia, P.M., Fritz, S.C., Baker, P.A., Seltzer, G.O., Dunbar, R.B., 2003. A Late Quaternary diatom record of tropical climatic history from Lake Titicaca (Peru and Bolivia). *Palaeogeogr. Palaeoclimatol. Palaeoecol.* **194** (1–3), 139–164.

Tatsumoto, M., Knight, R.J., Allègre, C.J., 1973. Time differences in the formation of meteorites as determined from the ration lead-207 to lead-206. *Science* **180**, 1279–1283.

Taylor, S.R., McLennan, S.M., 1985. *The Continental Crust: Its Composition and Evolution*. Blackwell, Oxford.

Taylor, S.R., McLennan, S.M., 1995. The geochemical evolution of the continental crust. *Rev. Geophys.* **33** (2), 241–265.

Tricca, A., Wasserburg, G.J., Porcelli, D., Baskaran, M., 2001. The transport of U- and Th-series nuclides in a sandy unconfined aquifer. *Geochim. Cosmochim. Acta* **65** (8), 1187–1210.

Turner, S., Van Calsteren, P., Vigier, N., Thomas, L., 2001. Determination of thorium and uranium isotope ratios in low-concentration geological materials using a fixed multi-collector-ICP-MS. *J. Anal. Atom. Spectrom.* **16** (6), 612–615.

Viers, J., Dupre, B., Polve, M., Schott, J., Dandurand, J.-L., Braun, J.-J., 1997. Chemical weathering in the drainage basin of a tropical watershed (Nsimi-Zoetele site, Cameroon); comparison between organic-poor and organic-rich waters. *Chem. Geol.* **140** (3–4), 181–206.

Vigier, N., Bourdon, B., Lewin, E., Dupré, B., Turner, S., Van Calsteren, P., Subramanian, V., Allègre, C.J., 2005. Mobility of U-series nuclides during basalt weathering: An example of the Deccan Traps (India). *Chem. Geol.* **219** (1–4), 69–91.

Vigier, N., Bourdon, B., Turner, S., Allègre, C.J., 2001. Erosion timescales derived from U-decay series measurements in rivers. *Earth Planet. Sci. Lett.* **193**, 546–563.

Whipple, K.X., 2001. Fluvial landscape response time: how plausible is steady-state denudation? *Am. J. Sci.* **301**, 313–325.